

1 **Transform margins of the Arctic: a synthesis and re-evaluation**

2 **A. G. Doré¹, E.R.Lundin², A. Gibbons³, T.O. Sømme³ & B.O. Tørudbakken³**

3

4 1. Statoil (UK) Ltd., One Kingdom Street, London W2 6BD, UK

5 2. Statoil Research Center, Arkitekt Ebbells veg 10, 7053 Trondheim, Norway

6 3. Statoil ASA, Drammensveien 264, Oslo 0283, Norway

7

8 **Abstract**

9 Transform margin development around the Arctic Ocean is a predictable geometric outcome of
10 multistage spreading of a small, confined ocean under radically changing plate vectors. Recognition
11 of several transform margin stages in Arctic Ocean development enables predictions to be made
12 regarding tectonic styles and petroleum systems. The De Geer margin, connecting the Eurasia Basin
13 (the younger Arctic Ocean) and NE Atlantic during the Cenozoic, is the best known example. It is
14 dextral, multi-component, features transtension and transpression, is implicated in microcontinent
15 release, and thus bears close comparison with the Equatorial Shear Zone. In the older Arctic Ocean,
16 the Amerasia Basin, Early Cretaceous counterclockwise rotation around a pole in the Canadian
17 Mackenzie Delta was accommodated by a terminal transform. We argue on geometric grounds that
18 this dislocation may have occurred at the Canada Basin margin rather than along the more distal
19 Lomonosov Ridge, and review evidence that elements of the old transform margin were detached by
20 Makarov-Podvodnikov opening and accommodated within the Alpha-Mendeleev Ridge. More
21 controversial is the proposal of shear along the Laptev-East Siberian margin. We regard an element
22 of transform motion as the best solution to accommodating Eurasia and Makarov-Podvodnikov
23 Basin opening, and have incorporated it into a three-stage plate kinematic model for Cretaceous-
24 Cenozoic Arctic Ocean opening, involving Canada Basin rotational opening at 125-80 Ma,
25 Makarov-Podvodnikov Basin opening at 80-60 Ma normal to the previous motion, and a Eurasia
26 Basin stage from 55Ma to present. We suggest that all three opening phases were accompanied by
27 transform motion, with right-lateral sense being dominant. The limited data along the Laptev-East
28 Siberian margin is consistent with transform margin geometry and kinematic indicators, and these
29 ideas will be tested as more data become available over less explored parts of the Arctic, such as the
30 Laptev-Eastern Siberia-Chukchi margin.

31

32

33 **Introduction**

34 The Arctic Ocean, essentially an enclosed ocean "at the top of the world" (Figures 1 & 2), is ice-
35 covered most of the year. For this reason, and because of inaccessibility and remoteness from major
36 habitations, the deep Arctic Ocean and its periphery remain poorly explored in both general and
37 geological terms. Compared to many of the world's oceans and margins, geological models are
38 poorly substantiated, many in number, and still essentially unresolved. In the last two decades,

39 however, geological understanding of the Arctic has improved and numerous geological studies have
40 been performed (see for example Geological Society Memoir 35, Spencer et al., eds., 2011). For
41 specific regions of the Arctic (e.g. Alaska, Barents Sea) a large body of literature is now available.
42 More remote areas, such as offshore eastern Siberia and the Chukchi Borderlands are far more
43 sparsely covered in terms of data and studies. Significantly, since Ziegler (1988) there have
44 been few pan-Arctic syntheses of geological development through time, with Golonka (2011) being
45 a notable exception.

46 The Arctic is also one of the few remaining underexplored petroleum provinces in the world, and is
47 considered by some authorities to house up to a quarter of the world's undiscovered resources (e.g.
48 Gautier et al. 2011). It is bordered by two of the world's major petroleum provinces (West Siberia
49 and Alaska's North Slope) and by unusually wide continental shelves (e.g. Barents, Kara and East
50 Siberian Seas) in the Norwegian and Russian sectors. Interest in the potential of the Arctic margins
51 was reflected in significant awards of prospecting rights offshore Russia, Norway and Greenland
52 between 2011 and 2013. The present paper, with its emphasis on the shear margins, is part of a
53 general update and petroleum geological synthesis of the Arctic carried out by Statoil in 2013-14,
54 taking in all seismic data, literature and studies in the company's database. The plate reconstructions
55 were performed with G Plates software (Boyden et al., 2011, Williams et al., 2012) in a global
56 EarthByte rigid plate model (based on Shephard et al., 2013).

57 At present day, limited connections exist between the Arctic Ocean and the Pacific Ocean and NE
58 Atlantic via the Bering and Fram Straits respectively (Figures 1 & 2). In the geological past,
59 likewise, the Arctic oceans have repeatedly been confined (e.g. Mann et al., 2009). The shape of the
60 Arctic Ocean generally reflects the underlying plate configuration, with oceanic crust (or, locally,
61 hyperextended continental crust or exhumed mantle) underlying the deep water areas. Large shallow
62 sea areas, such as the Barents and Kara Seas are underlain by continental crust. Although uncertainty
63 remains regarding the nature of the crust of some key Arctic elements, in particular the Alpha-
64 Mendeleev Ridge, most of the area can today be reasonably defined based on gravity, magnetics,
65 seismic refraction/reflection and outcrop data, and the interpretation can in turn be tested by plate
66 reconstructions.

67 The Arctic oceanic realm consists of the following major physiographic areas (Figures 1 & 2):
68 Canada Basin, Eurasia Basin, Makarov-Podvodnikov Basin, and fringing the central Arctic, the
69 northern part of the NE Atlantic and Labrador Sea-Baffin Bay. Internally to these are at least two
70 continental fragments, the Lomonosov Ridge and Chukchi Borderlands. Of more uncertain nature
71 are the Alpha and Mendeleev Ridges that lie within the Amerasia Basin (combined Canada Basin
72 and Makarov-Podvodnikov Basin), which may be entirely oceanic, or alternatively contain
73 continental material overlain by basalt flows and/or recent sediments. Although basalts cover these
74 ridges, extensional faults are quite widespread (e.g. Bruvold et al., 2012) and may reflect underlying
75 continental crust. Fairly well expressed continent-ocean-boundaries can be interpreted along the
76 Siberian and North American margins, the Lomonosov Ridge, the Chukchi Borderlands, and the
77 Barents-Kara Sea margin (Figure 3).

78 While numerous models exist for its opening and subsequent development, there is general
79 consensus that the Arctic Ocean is essentially a Late Mesozoic-Cenozoic feature, and that spreading
80 took place in several distinct stages (e.g. Churkin & Trexler 1980, Dutro 1981, Grantz et al., 1979,
81 Herron et al., 1974, Lawver et al, 2001). It lies between the Atlantic and Pacific, and compared to
82 these bordering pan-global oceans is a comparatively small ocean basin (Figure 1). Although
83 influenced by the development of both the Atlantic and Pacific, it has been a discrete and separate
84 entity for much of its existence. A natural concomitant of the size, multi-stage development and

85 isolated nature of the Arctic Ocean is that it must be bounded on several sides by transform margins.
86 Transform boundaries are common in plate tectonics and are fundamental to, and required by, plate
87 motions on a sphere. Plate separation motion is defined by rotation around a point on the surface, the
88 Euler pole, with the shear margin being a requirement at the distal end of the ocean from the pole. A
89 small, multi-stage ocean should therefore be characterized by several shear margins in relatively
90 close proximity to each other. What also typifies shear boundaries is that they, as well as oceanic
91 fracture zones, follow small circle arcs described by the respective Euler pole of rotation. Opening of
92 a small ocean around a nearby Euler pole will generate a pronounced V-shaped ocean and arcuate
93 fracture zones, whereas a very distant Euler pole may generate a slightly arcuate shear.

94 These geometries are all either observed or postulated in the Arctic (Figure 4). They include the
95 western Barents Sea margin, which includes major shear elements such as the Senja Fracture Zone
96 and Hornsund Fault, and links the NE Atlantic and Arctic. This margin is part of a major trans-
97 Arctic lineament sometimes termed the “De Geer Zone” (Harland 1965), which dates at least from
98 the closing stages of the Caledonian orogeny at approximately 400Ma. With the exception of the
99 Equatorial Shear Margin (e.g. Mascle et al., 1995, Nemčok et al., 2012 and papers in this volume)
100 this may be the best studied shear margin on the globe (e.g. Faleide et al., 2010, Gabrielsen et al.,
101 1990). The Eurasian side of the Amerasia Basin, generally (but not always) interpreted as a shear
102 margin (e.g. Grantz et al., 1979) is less well understood, in terms of both scale and position. In this
103 paper we also argue for the periodic existence of shear along the Siberian margin between the Laptev
104 and Chukchi Seas. Each of these proven or proposed shear margins is described below, after which
105 we integrate them into what we consider the most likely plate tectonic sequence of events. The sense
106 of shear in the Arctic appears to be overwhelmingly dextral, which may be coincidence or may
107 indicate a generic connection not yet clear to the authors. Additionally, an apparently intimate
108 relationship between the development of the shear margins and the formation of microcontinents is
109 evident in the Arctic, and appears to reflect a worldwide paradigm. This relationship is considered
110 in context below, but is also examined in a companion paper in this volume (Nemčok et al., this
111 volume).

112

113 **Principal structural units of the Arctic Ocean**

114 *Eurasia Basin*

115 The Eurasia Basin (Figures 1 & 2) is the prolongation of the Atlantic rift system, which through its
116 Mesozoic-Cenozoic evolution has nearly divided the Mesozoic Pangean supercontinent. Northeast
117 Atlantic-Eurasia Basin opening began at Isochron 24b-25 (54-56 Ma) time as the Nansen-Gakkel
118 Ridge formed between the Lomonosov Ridge microcontinent and the northern Barents-Kara Sea
119 margin. The two oceanic segments were linked by the De Geer transform margin until the end of the
120 Eocene (Isochron 13 time, 33 Ma). The Eurasia Basin largely consists of abyssal plain, with
121 maximum water depths between 4000 and 4500m. It is characterized by well-defined magnetic
122 isochrons that reflect the age of the ocean floor. Well-expressed isochrons are to be expected at a
123 high latitude, and the Arctic oceans have been at high latitude throughout their development. The use
124 of the isochrons establishes that the Eurasia Basin is the world's slowest spreading ocean (e.g. Snow
125 & Edmonds, 2007), and this fact has attracted a number of scientific studies, including sampling of
126 the seafloor (e.g. Michael et al., 2003). The continent-ocean boundaries (COB) against the Barents-
127 Kara margin and against the Lomonosov Ridge are well established by gravity, magnetic, and
128 bathymetry data. The COB against the rift tip in the Laptev Sea is also well established and
129 according to Drachev (1998), is marked by the Khatanga Shear or Severnaya Shear. The tectonic

130 implications of this major transform (shown as Khatanga-Bering Transform, KBT on Figure 2) have
131 not been widely discussed, and will be considered later.

132

133 *Lomonosov Ridge*

134 The Lomonosov Ridge (Figures 1 & 2) is an elongate feature of continental affinity extending 1800
135 km between the Canadian Arctic Islands and the Russian New Siberian Islands, and crossing the
136 North Pole. It rises to minimum depths of about 950m, is steep-sided and is bounded on each side
137 by the abyssal basins of the Eurasia Basin and the Amerasia Basin (Figure 1). The limited seismic
138 evidence shows that the ridge is multiply segmented, but in general contains relatively undisturbed
139 Cenozoic sediments overlying a faulted, presumed Mesozoic, basement (Jokat et al., 1992; Jokat,
140 2005). The ridge was cored by the ACEX (Arctic Coring Expedition) in 2004
141 (<http://www.ecord.org/pub/ACEX>), which found 420m of Cenozoic sediments, with the basal Early
142 Eocene-Paleocene sediments resting on an angular unconformity with underlying Mesozoic sands.
143 Of particular note is a major hiatus spanning from 44 to 18 Ma. (Moran et al., 2006). The
144 Lomonosov Ridge detached during the initial NE Atlantic-Eurasia Basin opening at Isochron 24b-25
145 (54-56 Ma) time (e.g. Brozena et al., 2003), as the Nansen-Gakkel Ridge formed between the
146 microcontinent and the northern Barents Sea margin. Its significance as the largest of the Arctic
147 microcontinents is discussed in Nemčok et al., (this volume).

148 *Amerasia Basin*

149

150 The Amerasia Basin (Figures 1 & 2) is far less understood. Although older and larger than the
151 Eurasia basin, water depths are somewhat lower, attaining a maximum of about 3900m. With a few
152 exceptions (Kristoffersen et al., 2008), the ocean floor is overlain by a very thick sedimentary
153 succession, preventing sampling of the seafloor. The Amerasia Basin is subdivided into the Canada
154 Basin and the Makarov-Podvodnikov Basin by an intervening diffuse rise, the Alpha and Mendeleev
155 ridge system (e.g. (Bruvoll et al., 2010; Jokat et al., 2013). Notably, neither of these oceanic realms
156 is characterized by well-defined magnetic isochrons. However, the Canada Basin has a well-defined
157 gravity anomaly in its centre (e.g. Grantz et al., 2011), generally accepted to be the abandoned
158 spreading axis. On either side of this axis is a single pair of magnetic isochrons. The pie-shaped
159 Canada Basin has been suggested to reflect counterclockwise rotational opening, whereby Alaska
160 (Figure 1) has moved away from the rifted Canadian margin. Carey (1958), well before acceptance
161 of plate tectonics, suggested that the swing in the Cordillera-Brooks Range represented an oroclinal
162 bend, i.e. a previously linear orogeny that became bent: this bend would now be viewed as
163 associated with the rotation of Alaska away from the Canadian Arctic margin. A number of other
164 plate models have been proposed (e.g. Churkin & Trexler 1980, Dutro 1981, Herron et al., 1974,
165 Lawver et al, 2001) but the “windshield wiper” model (Grantz et al., 1979) remains the most
166 generally accepted model for the Canada Basin. The amount of rotation, and the position of the
167 bounding shear (here termed the Amerasia Basin Transform, ABT on Figure 4) are considered
168 below.

169

170 The Makarov-Podvodnikov Basin is often ascribed a similar origin to the Canada Basin – i.e. formed
171 by rotation along with the entire Amerasia Basin (e.g. Grantz et al., 1979 & 1998). Herein, we treat it
172 as a separate basin analogous to the Eurasia Basin, although with its apex toward Greenland
173 and with a different and younger origin. These arguments are made in the section on the Amerasia
174 Basin Transform, below.

175

176 *Alpha-Mendeleev Ridge System*

177

178 The Alpha-Mendleev Ridge system (Figures 1 & 2) forms bathymetrically high elements, together
179 some 1500 km long and 250-400 km wide, rising 2 km above the adjacent Canada Basin and
180 Makarov-Podvodnikov Basins (Bruvoll et al., 2012). Strata subcrop directly at seabed on the Alpha
181 Ridge, but this area has some of the harshest ice conditions in the Arctic, and is difficult to access.

182

183 The ridge system appears to contain continental elements (Vernikovsky et al., 2013),
184 although velocity gradients from seismic refraction data also suggest an oceanic affinity and Bruvoll
185 et al. (2012) point to similarities with intra-plate oceanic volcanic constructs. The Alpha Ridge has
186 been proposed to be an element of an Arctic Large Igneous Province (LIP) formed at c. 125 Ma (e.g.
187 Lawver et al. 2002). However, very few samples exist of the basalt that is assumed to form the
188 acoustic basement. The only available geochronologic (Ar/Ar) date from the ridge is much younger -
189 Coniacian, 89 ± 1 Ma (Jokat et al., 2013). A limited number of piston cores from the Alpha Ridge,
190 collected from stations on the drifting Fletcher ice island in the late 1960s and 70s, reveal
191 Campanian to mid- Late Maastrichtian strata over acoustic basement (Jenkyns et al. 2004). Thus, the
192 limited sampled portion of the ridge appears to be Late Cretaceous in age, with Coniacian or older
193 acoustic basement and a sedimentary cover at least as old as Campanian. Both the Alpha and
194 Mendeleev Ridges are cut by normal faults and have a distinct horst-and-graben geometry. Bruvoll
195 et al. (2010) interpreted the age of faulting of the Alpha-Mendeleev Ridge to be Early Miocene, but
196 noted that there is no strong candidate regional tectonic event to which the deformation can be
197 linked. It appears possible that the extensional deformation is considerably older, since syn-
198 rift wedges are primarily observed in the succession immediately above acoustic basement
199 (basalt). A pronounced seabed relief of 500 m or more across some major normal faults
200 suggests recent reactivation.

201

202 *Other major elements of the Arctic*

203

204 The Chukchi Borderlands (e.g. Grantz et al, 2011; Houseknecht & Bird 2011) are a piece of
205 continental crust protruding into the Canada Basin from the westernmost part of Alaska (Figures 1 &
206 2). It rises very steeply from the abyssal plain to depths as shallow as 250m. In most reconstructions,
207 including that of this paper, formation of the Canada Basin by rotation of Alaska away from the
208 Canadian Arctic margin necessitates simultaneous rotation the Borderlands from a position parallel
209 with the Alaska margin. This rotation has the opposite sense to the general rotation of Alaska, i.e.
210 while the Canada Basin formed by counterclockwise rotation of Alaska away from the Canadian
211 Arctic margin, the Borderlands rotated clockwise away from East Siberian margin. In this
212 interpretation the North Chukchi Basin, in the space between the Siberian margin and the
213 Borderlands created by the rotation, would probably be floored by either exhumed mantle or by
214 oceanic crust. The extreme depth of the sedimentary basin, up to c. 18-20 km, has been remarked
215 upon by Drachev (2011). Note, however, that a more radical interpretation by Nikishin et al. (2014)
216 places the Amerasia Basin Transform (ABT, Figure 4) along the North American flank of the
217 Borderlands, which would therefore not be rotated. Ultimately, only palaeomagnetic work on
218 orientated cores from the sparsely-studied Borderlands is likely to resolve this issue.

219

220 The Morris Jessup and Yermak Plateaux (Figure 2) are paired, probably incipient microcontinental
221 elements either side of the Fram Strait, which separates Greenland and Spitsbergen and links the
222 Atlantic and Arctic oceans. The Yermak Plateau extends northwards from western Spitsbergen into
223 the Eurasia Basin as a shallow area of sea floor, and has variously been interpreted as a continental
224 fragment (e.g. Jokat et al., 2008) or anomalously shallow ocean floor derived from hotspot activity
225 (Feden et al., 1979). The Morris-Jessup Rise on the opposing side of the Eurasia Basin is its mirror-
226 image, and these features are cut off by post-Isochron 13 ocean floor, implying that the two plateaux
227 were a single plateau prior to separation at the Eocene-Oligocene transition. The Yermak Plateau

228 shows indications of late volcanism (Geissler et al., 2011), probably representing the propagation
229 and conjoining of the Knipovitch (Atlantic) and Gakkel (Eurasia basin) ridges during the onset of
230 passive drift.

231

232

233 **Shear margins, proven and postulated**

234

235 *De Geer transform margin*

236

237 The De Geer line or zone was a term coined by Harland (1965) for the remarkably straight lineament
238 cutting across the Arctic from the northern coast of Norway, along the Svalbard and Greenland-
239 Canadian Arctic margin, to the Mackenzie Delta, a distance of some 4000 km (Figures 2 & 3). The
240 lineament is evident in the trend of the continental margins, in component NNW-SSE shear faults
241 linking the NE Atlantic and Arctic (e.g. Hornsund Fault, Senja, Spitsbergen and Greenland fracture
242 zones), and in major margin-parallel fractures on the western Barents shelf and on Spitsbergen (e.g.
243 Gabrielsen et al., 1990; Worsley & Aga 1986).

244

245 This transform margin links two major Cenozoic ocean basins, the Northeast Atlantic and the
246 Eurasia Basin of the Arctic Ocean. However, the greater De Geer zone almost certainly exploited a
247 Paleozoic zone of weakness dating at least from the Caledonian orogeny at approximately 400Ma at
248 the Silurian-Devonian transition (e.g. Harland, 1965; Faleide et al., 1993) (Figure 5). This event was
249 the culmination of a long sequence of terrane accretion, finally resulting in the closure of the ancient
250 Iapetus Ocean and the fusing of Baltica (mainland Norway, Sweden) with Laurentia (Greenland,
251 North America). The Inuitian fold belt (Figure 5) running through Spitsbergen, North Greenland and
252 Arctic Canada, is broadly contemporaneous with the Caledonian deformation (e.g. Ohta et al. 1989)
253 and suggests that the NE-trending orogen turned NNW at the present Barents margin, or that the
254 Inuitian was an important side-branch of the orogen. (e.g. Gee & Teben'kov 2004). A final phase of
255 the Caledonian, the Svalbardian, took place in Late Devonian times. This phase has been proposed to
256 represent major strike-slip along the line of the Caledonian-Inuitian orogen and the assembly of
257 Svalbard from sinistral movement of originally widely separated terranes (e.g. Harland 1965). The
258 magnitude and complexity of this movement is still a matter of debate (Torsvik 1985; Gee &
259 Teben'kov 2004). Critical for the later transform margin evolution, however, is the fact that this late
260 movement involved a series of extensive NNW-trending lineaments such as the Billefjorden Fault
261 Zone on Spitsbergen, which were repeatedly reactivated through later geological time and defined
262 the western margin of the Barents Sea.

263

264 A probable sequence of Cenozoic break-up events linking the NE Atlantic and Eurasia Basin is
265 shown in Figure 6, adapted from the work of Faleide et al. (2010) and others. On the Mid-Norway
266 and East-Greenland margins, separation to form the Mohn's Ridge in the Early Eocene (Isochron 24b
267 time, 54 Ma) was predated by a period of crustal extension in the latest Cretaceous and Paleocene
268 (e.g. Ren et al. 2003), accompanied by extensive basaltic magmatism. As break-up progressed, a
269 dextral transform margin developed along the western Barents Sea margin, accompanied by severe
270 contractional movements in the north and the formation of the West Spitsbergen fold and thrust belt,
271 which extended northwestwards into the Eurekan fold belt of northern Greenland and Arctic Canada
272 (see full description in Dallmann et al. 1993). The fold belt is usually dated as Paleocene to Eocene,
273 but has also been suggested to have originated in the Late Cretaceous (Lyberis & Manby 1993),
274 synchronously with contractional movements in the Wandel Sea Basin, North Greenland. The
275 Paleocene-Eocene Central Basin of Spitsbergen developed immediately west of the Billefjorden

276 Fault Zone, as a foreland basin to the fold belt to the west, but also possibly as a response to pull-
277 apart. Simultaneously, sedimentary basins probably attributable to pull-apart were formed on the
278 southwestern Barents Sea margin: the Sørvestnaget Basin and Vestbakken Volcanic Province (e.g.
279 Gabrielsen et al., 1990). The transit of a spreading ridge along the transform margin a short distance
280 west of these basins gave rise to volcanism in the Vestbakken Volcanic Province between the
281 Eocene and earliest Oligocene. Episodes of compressive stress occurred contemporaneously in the
282 two basins, forming NW-SE trending intra-basinal folds and hanging wall anticlines. This complex
283 interrelationship of Paleogene basins and highs along the western Barents Sea margin is illustrated in
284 Figure 7.

285

286 At the Eocene-Oligocene transition (Isochron 13 time, 33 Ma) a significant change in the pole of
287 rotation occurred such that the NW-directed spreading changed to a more westerly course (e.g.
288 Faleide et al., 2010). This resulted in the propagation of the Knipovitch Ridge between the Mohns
289 and Nansen-Gakkell Ridges, and the separation of Greenland from the Barents margin. The change to
290 passive drift terminated the West Spitsbergen compressional episode and brought a period of
291 tectonic quiescence to the western Barents Sea. It is generally thought that at this stage, fragments of
292 the former transform margin, the Hovgaard Ridge and the East Greenland Ridge along the northern
293 part of the Greenland Fracture Zone, were separated from the Barents Sea margin and drifted
294 westward as the Knipovitch Ridge spreading continued (e.g. Myhre & Thiede 1995; Døssing &
295 Funck 2012). The true picture may, however, be more complicated. As pointed out by Myhre &
296 Eldholm (1988) and others, it is likely that the microcontinental slivers were involved in a complex
297 northeastwards propagation of the NE Atlantic via small spreading cells that may have begun as
298 early as Isochron 22 time (50 Ma), and were rifted away from the Barents-Svalbard margin prior to
299 the full development of the Knipovitch spreading ridge (Figures 6 & 7: see also Nemčok et al., this
300 volume).

301

302 The apparent extension of the De Geer Line along the Greenland-Canada Arctic margin could of
303 course be a coincidental alignment. More likely, however, is that a general zone of shear existed in
304 this region in the Paleozoic, associated with the NNW turn of the Caledonian orogen into the
305 Inuitian system (e.g. Ohta et al., 1989; Gee & Teben'kov 2004). In the Canadian Arctic islands, the
306 straight continental margin forms the northern limit of the Inuitian fold belt and is paralleled inboard
307 by the Sverdrup Rim, an elongate basement high forming the northern boundary of the Late
308 Paleozoic-Mesozoic Sverdrup Basin. These lineaments separated the Canada margin from Crocker
309 Land, a significant terrane and source area to the Sverdrup Basin, generally presumed to be part of
310 the Chukotka terrane now incorporated into the Siberian shelf (e.g. Embry & Beauchamp 2008).
311 This unit was rotated away from the Canadian margin in the Early Cretaceous during the opening of
312 the Canada Basin (see following section and Figure 6). It is thus quite plausible that early
313 development of the Arctic Ocean (as well as the Cenozoic development) was facilitated by
314 continental separation along the former shear zone. If this argument is accepted, the De Geer zone
315 can claim a major role in the mega-structural history of the Arctic from the Caledonian to the
316 present, and has been involved in orogen-parallel shear, fold-and-thrust belts, convergent and pull-
317 apart basins, volcanism, microcontinent release and passive plate separation

318

319

320 *The Amerasia Basin Transform*

321

322 The rotational model for the initial opening of the Amerasia Basin (Grantz et al, 1979) involves the
323 rotation of a microcontinental block (Chukotka) away from the Canadian Arctic margin. As
324 indicated above, this idea is widely accepted because of the relic spreading ridge detected on gravity
325 data, the two paired apparent magnetic anomalies either side of it, and the generally triangular nature

326 of the Canada Basin (Figures 2 & 8). The Canadian apex of this triangle lies in the Mackenzie
327 Delta, representing the likely pole of rotation. While Grantz et al., (1979) and many other subsequent
328 authors describe a c. 66° rotation around the pole, it is debatable how much of this opening
329 represents true oceanic spreading. One view with a strong circumstantial basis is that the general
330 absence of magnetic anomalies indicates spreading during the Cretaceous “quiet zone” (118-84 Ma).
331 By this hypothesis, the single pair of anomalies would indicate a cessation of spreading at about 80
332 Ma, just after the reappearance of magnetic reversals. However, it is known that the margins of the
333 Canada Basin represent initial slow spreading, are magma-poor and likely to feature wide zones of
334 exhumed mantle (e.g. Grantz et al, 2011 and in-house potential fields modelling). This may provide
335 another explanation for the absence of linear anomalies. A recent model for the Arctic Ocean
336 (Nikishin et al., 2014) focuses on the idea that the few central anomalies may represent a very
337 limited spreading cell, with the remainder of the basin constituting foundered, hyperextended
338 continent or exhumed mantle. However, we favour the wider, c. 66° rotation because of overall fit
339 with the basin shape, general Arctic kinematics (including the Alaskan oroclinal bend) and
340 independent paleomagnetic evidence of rotation of Alaska (Halgedahl & Jarrard, 1987).

341 Timing of crustal separation in the Canada Basin (whether by mantle exhumation or oceanic
342 spreading) is, for similar reasons not accurately known. Wells along the Canadian Arctic, Beaufort-
343 Mackenzie and North Slope margins constrain the pre-breakup rifting to Kimmeridgian through to
344 Hauterivian (e.g. Dixon 1982). The Hauterivian unconformity is a pronounced regional break along
345 the Canada Basin margins and marks the upper limit of rifting. Rifting of continents typically
346 becomes younger towards the location of continental separation, and hence we deduce that the
347 Hauterivian is a lower limit for break-up. Dike swarms and lava flows in the Canadian Arctic
348 margin, Svalbard, Frantz Josef Land, and southern East Siberian Islands indicate a peak of
349 magmatism at c. 125 Ma, i.e. at the end of the rift episode (in-house analysis and Corfu et al., 2013).
350 This volcanism may therefore be associated with the initial Arctic break-up event, leading us to a
351 best-guess interval of 125-80 Ma for the Canada Basin rotation.

352 The terminal shear of the rotational opening or "windshield wiper shear" must of course have been a
353 transform margin during the Early Cretaceous, and like the De Geer Zone the sense will have been
354 right-lateral (Figure 8). Grantz et al. (1979) proposed that this shear followed the edge of the
355 Lomonosov Ridge (on the Canada Basin side) and continued into Siberia. The shear is generally
356 terminated against the western tip of the South Anyui suture (Figure 8), a diffuse tectonic break
357 associated with folding, thrusting and ophiolites (e.g. Sokolov et al, 2009) representing closure of a
358 former oceanic element of the Pacific, the South Anyui Sea. The Canada Basin would thus have
359 opened in concert with closure of the South Anyui Sea, so that the "windshield wiper" shear did not
360 cut across Siberia to the Pacific plate, but instead continued into the suture between Chukotka and
361 mainland Siberia.

362 A problem with this proposed location for the transform margin is the linear, non-curved nature of
363 the Lomonosov Ridge. If its Amerasian flank marks the paleo-shear margin, it is neither sufficiently
364 arcuate to correspond to the small circle centered about the Euler rotation pole in the Mackenzie
365 Delta area (MD, Figure 2), nor to have been defined by the relic spreading ridge. This geometric
366 problem has been pointed out by other authors (e.g. Rowley & Lottes 1988, Kuzmichev 2009) and
367 alternative models involving a shear traversing the Siberian shelf in a more easterly position have
368 been suggested (Figure 8). The validity of these alternatives hangs on the nature of the South Anyui
369 Suture and basement structural continuity across the Siberian shelf.

370 Both seismic and sampling data are very sparse on the shelf, but outcrops have been studied on the
371 New Siberian and De Long islands between the Laptev and East Siberian seas. Kuzmichev (2009)

372 asserts that field evidence points to extension of South Anyui deformation offshore and as far west
373 as Big Lyakhovsky Island (Figure 8), a view supported by the maps of Vernikovskiy et al., (2013a).
374 Given a simple one-to-one relationship between the suture and the rotational shear, this evidence
375 would push the shear westwards and support the correlation with the Lomonosov Ridge. However,
376 as shown by Figure 8, Sokolov et al., (2002) and Vernikovskiy et al., (2013a), the suture zone is
377 anything but simple, recording a history of terrane and ophiolite accretion on the margins of the
378 South Anyui Sea dating back to the Late Paleozoic. Additionally, almost synchronously with the
379 assumed collision of the rotating Chukotka block with Siberia in Early Cretaceous times, a further
380 large terrane (Kolyma-Omolon) impinged westwards on the continent from the paleo-Pacific (e.g.
381 Shephard et al., 2013), forming the Verkhoyansk Foldbelt immediately south of the present Laptev
382 Sea (Figure 8). The close proximity and co-evolution of these elements illustrates the complexity of
383 the Eastern Siberian plate tectonic collage, and the probable over-simplified nature of the rotation-
384 collision model. The occurrence of major dextral shear along the line of the South Anyui Suture, as
385 proposed by Sokolov et al., (2002), would further blur the entry position of the Amerasia Basin
386 Transform.

387 Paleomagnetic work by Vernikovskiy et al. (2013a & b) demonstrates apparent basement continuity
388 between the New Siberian and De Long islands, and thus that a major shear is unlikely to have
389 interposed between the two archipelagos. A clinching piece of evidence - for the position of the
390 main transform west of the New Siberian Islands and the amount of lateral translation - would be
391 paleomagnetic or polar wander data placing the islands adjacent to the Barents Sea Svalbard margin
392 prior to rotation. To our knowledge, however, no such data exists.

393 A different location of the transform, closer to the Alpha Ridge (Figure 8), would allow a more
394 arcuate margin, corresponding better with the Canada Basin rotation. This interpretation implies that
395 the Makarov-Podvodnikov Basin, located between the Lomonosov Ridge and the Alpha-Mendeleev
396 Ridge, would include separate oceanic elements formed between cessation of Canada Basin rotation
397 and Eurasia Basin initiation. Like the Eurasia Basin, opening would have been orthogonal to the
398 Canada Basin spreading. A similar interpretation has been proposed by Arctic workers repeatedly in
399 the past (e.g. Taylor et al., 1981, Drachev et al., 1998, Franke et al., 2004, Rowley & Lottes 1988,
400 Sekretov 2001).

401 As indicated earlier, the curious array of normal faults cutting the Alpha-Mendeleev Ridge area
402 (Bruvoll et al., 2010) currently lacks a candidate regional tectonic phase. The faults were active in
403 the Cenozoic but, significantly, offset the acoustic basement with basal syn-rift wedges, and thus
404 probably have an older origin. If this is the case, a best-fit timing for the faults may be the rift phase
405 immediately preceding Makarov-Podvodnikov Basin opening, with some continental material
406 entrained in the Alpha-Mendeleev Ridge, and with the Coniacian volcanic dates on the ridge (Jokat
407 et al., 2013) representing pre-opening volcanism.

408 In summary, the sparse geophysical and geological data allows a wide range of interpretations for
409 the location of the Amerasia Basin rotational transform margin. Our preferred view is that the
410 Alpha-Mendeleev Ridge marks the approximate location of the shear, albeit subsequently
411 significantly blurred by the volcanic signature. We favour this interpretation on the basis of
412 geometries and kinematics, which become even more self-consistent if it is accepted that the
413 oceanward position of the transform was displaced westwards along the Siberian margin by
414 Makarov-Podvodnikov and Eurasia Basin spreading (see arguments below). Elements of the
415 transform margin probably flaked off as microcontinents during Makarov-Podvodnikov rifting and
416 spreading, and are now entrained in the Alpha-Mendeleev Ridge. Constrained by the age of the
417 volcanics, and bracketed by Canada Basin and Eurasia Basin spreading episodes, Makarov-

418 Podvodnikov Basin opening probably took place in the Late Cretaceous at c. 80 Ma and lasted until
419 c. 60 Ma. Margin-parallel shears probably helped to define the elongate Lomonosov Ridge
420 microcontinent, but this feature essentially reflects the trend and spreading vector of the Nansen-
421 Gakkel spreading ridge and can perhaps be regarded more as a product of detachment during Eurasia
422 Basin formation, rather than a precise proxy for the paleo-transform margin.

423 *Shear geometries on the Siberian-Alaskan margin*

424 Whilst it is clear that the Laptev rift system is the tip of the Eurasia Basin, there appears to be a
425 marked and abrupt discrepancy in extension between the oceanic domain and the rift. This is well
426 expressed by the bathymetry. We argue below that the two domains are separated by a major
427 transform.

428 The total width of the Laptev rift system as it abuts the Eurasia Basin is approximately 750 km (Figs.
429 9a and 9b), and while seismic refraction data reveal significant crustal thinning under the most
430 extended parts of the rift (Fig. 11), the crustal thinning is generally no more than ca 50% on average
431 (D. Franke, Personal Communication, 2014). The width of the oceanic crust of the Eurasia Basin
432 when it abuts the Laptev rift is approximately 600 km (Figs. 9a and 9b). In addition to this amount of
433 plate separation, the bordering rifted margins must have been extended prior to break-up. A necking
434 width of c. 100 km is probably reasonable, yielding a total extension in the Eurasia Basin just north
435 of the proposed transform in the order of 700 km.

436 Rigid-plate reconstructions have been proposed that require approximately 600 km of
437 extension in the Laptev rift (Gaina et al., 2002), a value also adopted by Shephard et al., (2013).
438 However, this amount of extension appears difficult to document for the Laptev rift system. Gravity
439 inversion (Alvey et al., 2008; Wienecke et al., 2011) reveals a remaining crustal thickness in the
440 Laptev rift of approximately 20 km (Fig. 3), which is approximately what is revealed by refraction
441 data (e.g. Franke et al., 2001) (Fig. 11). Summed fault heaves reveal even less extension (Fig. 11).
442 In-house subsidence analysis and forward modelling based on summed fault heaves interpreted from
443 seismic data suggest a stretching factor of approximately 1.25 (R. Kyrkjebø, Personal
444 Communication, 2015). Given a total width of the Laptev rift system of c. 750 km just south of the
445 Eurasia basin margin (excluding the Laptev horst) (Figs 9a and 9b), and a stretching factor of 2
446 (based on the remaining crustal thickness), this suggests that the rift has experienced no more than c.
447 350 km of extension where it is widest near the ocean margin. A recent extension estimate from
448 gravity modelling (Mazur et al., 2015) suggests a larger extension value, in the order of 500 km, in
449 the Laptev rift system. Such extension would probably imply hyperextension and complete absence
450 of crust in places, an observation that appears to be in conflict with the shallow, shelfal water depths
451 of the present day Laptev Sea (10-50 m). We note that this estimate hinges strongly on an assumed
452 original crustal thickness of 40 km and appears to be measured on lines that run quite obliquely to
453 the rift. Furthermore, this work assigns extension to both the Cretaceous and Cenozoic, and since the
454 Eurasia Basin extension is entirely Cenozoic in age this would increase the Cenozoic discrepancy
455 between the Eurasia basin and Laptev Shelf. Thus, at least for the Cenozoic, the Mazur et al. (2015)
456 extension value appears to be an overestimate.

457 We conclude that approximately half of the extension required to open the Eurasia Basin remains
458 unaccounted for in the Laptev rift. This discrepancy has previously been pointed out, particularly by
459 Drachev and co-workers (e.g. Drachev 1998, Drachev et al., 2003, Franke & Hinz, 2005, Drachev
460 2011), but has generally been overlooked in plate kinematic reconstructions.

461 A zone of strike-slip motion between the Laptev Rift and Eurasia Basin, marked by both the abrupt
462 bathymetric change and by a long lineament on the Bouger Anomaly map (Figure 9a), is the most
463 likely explanation for the discrepancy, and is probably necessary for a geometrically satisfying plate
464 model. A shear directed westward into the Yenisey-Khatanga Trough (Figure 2), eastward along the
465 East Siberian margin, or both, has long been suggested and has been named the Khatanga Shear
466 (Drachev, 1998), the Severnyi Transfer (Fujita et al., 1990), and the Khatanga-Lomonosov shear
467 (Drachev, 2011). The Yenisey-Khatanga Trough, and the major West Siberia Basin at its western
468 end are characterized by anticlines (Vyssotski et al., 2006) and strike-slip indicators (Gogonenkov &
469 Timurziev 2012), both of which may in part represent accommodation of Arctic Cenozoic spreading
470 in the Russian continental interior. In modern times a magnitude 6 earthquake with a strike-slip
471 focal plane solution occurred along the proposed shear in the Laptev Sea (Franke et al., 2004). This
472 type of structure is by no means unusual at the tip of propagating oceans. A strongly analogous case
473 is the northern Red Sea, which is separated from the much less extended Gulf of Suez by the sinistral
474 Dead Sea Transform (e.g. Freund 1970, Steckler & ten Brink 1986, Figure 12).

475 As argued above and by Taylor et al., (1981), Drachev et al., (1998), Franke et al., (2004), Rowley
476 & Lottes (1988) and Sekretov (2001), the Makarov-Podvodnikov Basin can be regarded as separate
477 from, and younger than, the remainder of the Amerasia Basin (i.e. the Canada Basin). The spreading
478 vector would have been almost normal to that of the Canada Basin, analogous to the Eurasia Basin,
479 although with the apex of the ocean towards Greenland and its broader distal margin towards East
480 Siberia. This interpretation would predict i) shear margin architecture along the East Siberian margin
481 and ii) precursor rifts to Makarov-Podvodnikov spreading on the adjacent East Siberian shelf,
482 subsequently abandoned as the Late Cretaceous transform margin developed. These geometries have
483 both been described by Sekretov (2001) (Figure 13). It is important to note that data is extremely
484 sparse in this area, limited to regional potential fields and a few regional seismic lines across the
485 margin and internal shelf. Nevertheless, in-house study and Sekretov's observations both suggest
486 that the East Siberian margin, although now overstepped by thick Cenozoic sediments, was faulted
487 and steep in the Cretaceous (Figure 13), a geometry characteristic of transform margins where abrupt
488 crustal attenuation rather than gradual necking towards the ocean is typical (e.g. Mascle et al., 1995;
489 Nemčok et al., 2012). At least two rifted and lightly inverted basins occur on the interior shelf,
490 consistent with extension and later shear.

491 Shear along the Siberian Margin would have been relayed, again by right lateral motion, into the
492 Chukchi Sea-Bering Strait region (Figure 9). As the plate reconstructions will show, this is an
493 attractive solution since it restores Wrangel Island and the Brooks Range, and they in turn become
494 aligned with the North American Cordillera when the Canada Basin is closed. The possible
495 continuity between the Brooks Range and Wrangel Island has previously been remarked upon
496 (Moore et al., 2002; Miller et al, 2006), but has remained controversial because the two are offset,
497 dextrally, by c. 600 km. Arctic Ocean kinematics and right-lateral marginal shear provides a
498 potential solution to this offset. Shear may have run along (and/or been expressed as) the Wrangel-
499 Herald Arch, an offshore basement high and deformation zone running NE-SW between Wrangel
500 and the Lisburne Hills at the western tip of the Alaska Peninsula (Verzhbitsky et al., 2008). Shear
501 may also have exited the Arctic Ocean into the Pacific via the present day Bering Strait, where the
502 position of the Mesozoic-Cenozoic Long Strait and Hope Basins again appear to show dextral offset.
503 Potentially, both lineaments exist as splays where the shear margin dissipates into Alaska and the
504 Pacific. A well-defined shear, probably dextral, running along the northern end of the Hanna Trough
505 in the Alaskan Chukchi Sea, may be a further splay of the Khatanga-Bering Transform. It is
506 expressed as a steep flower structure observed on seismic data. A dense "orthorhombic" conjugate
507 fault set of Late Cretaceous-Early Cenozoic age mapped on 3D seismic immediately south in the
508 Hanna Trough is usually attributed to 3D strain in a strike-slip regime (c.f. Krantz 1988), although

509 the origin of such lateral motion has not been clear. The model of dextral shear along the margin
510 related to Makarov-Podvodnikov and Eurasia Basin spreading provides a potential explanation for
511 the orthorhombic faults. A testable hypothesis is that similar fault sets will be identified in the cover
512 successions of other basins along the sheared Siberian margin as better data sets become available.

513 Our proposal therefore is that most of the Laptev and East Siberian Arctic COBs existed as
514 transform margins for at least part of their geological history. On Figure 9 we show this margin as a
515 composite or contiguous transform, which have termed Khatanga-Bering Transform. It is quite
516 plausible however that two separate shears exist, one relaying Late Cretaceous Makarov-
517 Podvodnikov and Cenozoic Eurasia Basin spreading dextrally via western Alaska and the Bering
518 Strait into the Pacific, and one relaying Eurasia Basin spreading sinistrally via the Yenisey-Khatanga
519 Trough into Western Siberia, as implied by Drachev (1998). In general, this zone can be viewed as
520 the northernmost, terminating transform margin of Atlantic spreading, a trans-global system
521 characterized by multiple major transform zones, generally dextral, separating oceanic segments of
522 differing ages (Figure 14).

523

524 **Opening of the Arctic Ocean in a regional transform setting**

525 We have argued above that shear margins are commonplace around the Arctic, and are an inevitable
526 product of accommodating opening along several vectors in a small, confined ocean. In this section
527 we use these arguments to propose an integrated kinematic history, illustrated stepwise in Figures 15
528 to 18. The present day position of the main plate tectonic elements is shown in Figure 15. As we
529 have been careful to point out, all of these kinematic elements including 3-stage models (e.g. Alvey
530 et al., 2008) have been described in the Arctic literature, albeit not in this particular combination and
531 timing, and with less emphasis on shear along the Laptev-Siberian continental margin.

532 ***Canada Basin stage 125-80 Ma***

533 In the 125 Ma reconstruction (Figure 16) the Brooks Range and Wrangel Island are aligned with the
534 trend of the North American Cordillera, i.e. predating the oroclinal bend that was imposed as
535 Alaska-Chukotka rotated counter-clockwise away from the Canadian Arctic margin. Breakup-
536 related mafic magmatism (red stars on Figure 15) occurred in the Sverdrup Basin area, Svalbard,
537 Franz Josef Land, and East Siberian Islands, which all restore closely together (e.g. Corfu et al.,
538 2013). Subduction and terrane accretion was taking place along the paleo-Pacific margin. The South
539 Anyui Sea – the space into which Chukotka-Alaska rotated – was present as an embayment in the
540 Pacific margin. Interestingly, the South Anyui Sea lines up rather precisely with the Uralian orogen,
541 the largely Late Paleozoic fold and thrust belt representing closure between Siberia and Baltica (e.g.
542 Puchkov 2009). This connection is also implicit in the reconstructions of Sokolov et al., (2002),
543 which also demonstrate the Late Paleozoic initiation of the South Anyui Suture. The last
544 compressional activity took place in Triassic-Jurassic time, recorded in the northernmost outpost of
545 the Uralian chain, the Taimyr Peninsula and the adjacent Yenisey-Khatanga Trough (e.g.
546 Kontorovich et al., 2013). The South Anyui Sea can perhaps, therefore, be regarded as an imperfect
547 join between Baltica and Siberia that was annealed as subduction consolidated along the Pacific
548 margin, with the early Arctic Ocean being a product of this reorganization.

549 Continued widening of the Canada Basin (100 Ma reconstruction, Figure 16) was accommodated by
550 translation along the major dextral transform at the distal end of the Canada Basin as the South
551 Anyui Sea was gradually subducted beneath the Chukotka terrane, with associated deformation

552 along the South Anyui suture (e.g. Sokolov et al., 2009). The Brookian orogeny of Alaska began
553 with accretion of island arcs to the North American Plate in the Jurassic, but the main crustal
554 thickening in the Brooks Range occurred in the Early Cretaceous (e.g. Toro et al., 2002; Bird &
555 Houseknecht 2011). The compression was driven by subduction on the Pacific side. However,
556 simultaneous opening of the Canada Basin in the Early Cretaceous probably played a role in the
557 deformation, and the Brooks orogeny can be viewed as part of the same general system of terrane
558 consolidation that affected the South Anyui suture.

559 Simultaneously the future Chukchi Borderlands detached from the Canadian margin and rotated
560 clockwise away from the East Siberian margin. Initially, the Borderlands formed a bridge between
561 the Arctic Canadian margin and East Siberia, but continued opening of the Canada Basin resulted in
562 cessation of Borderlands rotation, drifting away from the Canadian margin and development of the
563 single through-going spreading axis that is seen abandoned today. By 90 Ma the Canada Basin was
564 nearly completely open and the South Anyui Sea nearly completely subducted. A basaltic magmatic
565 pulse around 80-90 Ma (red stars, Figure 17), affecting the eastern Sverdrup Basin (e.g. Døssing et
566 al., 2013) and Alpha Ridge (Jokat et al., 2013), heralded opening of the Makarov-Podvodnikov
567 Basin (respectively SB, AR and MPB, Figure 2).

568 ***Makarov-Podvodnikov Basin stage 80-60 Ma***

569 At 80 Ma (Figure 17) the Canada Basin spreading had terminated, and the Makarov-Podvodnikov
570 Basin started to break up with an axis almost normal to the Canada Basin spreading centre. Viewed
571 on the large scale, the radical change in spreading vector can be regarded as propagation of Atlantic
572 Pangean break-up northwards into the Arctic; specifically the Makarov-Podvodnikov Basin may
573 have linked with the northward propagating Labrador Sea-Baffin Bay system. Initial rifting took
574 place in the Labrador Sea in the Barremian and in Baffin Bay in the Aptian-Albian, followed by
575 break-up, with mantle exhumation, in the Late Cretaceous, leading eventually to the first proper
576 oceanic crust in the Paleocene around 61 Ma (Balkwill 1987; Larsen et al., 2009; Harrison & Brent
577 2011). Makarov-Podvodnikov opening may also have linked with latest Cretaceous extension on the
578 margins of the developing NE Atlantic rift between Greenland and northern Norway (e.g. Ren et al.
579 2003).

580 As the Makarov-Podvodnikov Basin formed, volcanic constructs and continental fragments were
581 rifted away from the former sheared margin of Canada Basin and incorporated into the Alpha-
582 Mendeleev Ridge. Opening was relayed by right-lateral transform motion along the Siberian margin
583 towards the Pacific margin, probably exiting the Arctic Ocean via the present day Bering Strait but
584 with splays through the Wrangel-Herald Arch and north of the Hanna Trough. Wrangel Island and
585 the Brooks Range gradually became more displaced from one another. In our model, the major plate
586 motion at this time was assigned to Eurasia (reaching the active Tethyan margin) rather than North
587 America, to avoid implying compression in the region of the Canada Basin margins. By 70 Ma the
588 Chukotka orogen was no longer active and the South Anyui Suture was completely closed. There
589 was also a cessation in activity on the Brooks Range orogen, but activity was renewed at c. 60 Ma
590 (Late Brookian event), with the shedding of thick sediments northwards into its foreland basin, the
591 Colville Trough (e.g. Houseknecht & Bird 2011).

592 A major basaltic magmatic pulse in the interval 62-58 Ma spanning 2000 km between Disco Island,
593 Baffin Bay and the British Volcanic Province (e.g. Saunders et al. 1997) is generally taken to be the
594 precursor of NE Atlantic spreading (see 60 Ma reconstruction, Figure 17). Notably however, the
595 orientation of this magmatic belt was nearly perpendicular to the evolving NE Atlantic rift (e.g.
596 Smallwood & White 2002, Lundin & Doré 2005).

597 ***NE Atlantic-Eurasia Basin stage 55-0 Ma***

598 Opening of the NE Atlantic and Eurasia Basin is well established from magnetic isochrons in the NE
599 Atlantic, ODP drilling of seaward-dipping reflectors marking the mid-Norwegian COB (Eldholm et
600 al., 1989) and off SE Greenland (e.g. Larsen & Saunders 1998), and numerous other scientific
601 studies. This event was marked by a pulse of magmatism between c. 56 and 53 Ma (e.g. Saunders et
602 al., 1997). From 55 to 33 Ma both the Labrador Sea and NE Atlantic opened on either side of
603 Greenland (see 33 Ma reconstruction, Figure 18). The simultaneous opening on two arms of
604 spreading caused Greenland to move northwards, leading to collision between Greenland and
605 Ellesmere Island in the Canadian Arctic (Eurekan Orogeny), and transpression between Greenland
606 and Svalbard (West Spitsbergen Orogeny) associated with dextral translation along the NNW-SSE
607 De Geer shear zone.

608 The relaying of motion between Baffin Bay and the Eurasia Basin is enigmatic. Baffin Bay
609 terminates rather abruptly to the north, beyond which only small half-grabens exist in Lancaster and
610 Jones Sounds. Accommodation of Labrador Sea-Baffin Bay opening has traditionally been
611 visualized as the “Wegener Fault” (e.g. Harland 1965), a NE-SW sinistral shear, running along the
612 Judge Daly Fault in the Nares Strait (e.g. Figures 2, 17 & 18). However, despite the Nares Strait
613 forming an impressive NE-SW lineament, recent work on piercing points across the strait suggests
614 limited lateral movement (Harrison 2004). Since the existence of shear is necessitated by the
615 opening of an oceanic basin (on a sphere) in a rigid plate model, the best candidate location for this
616 movement is within the Eurekan foldbelt on Ellesmere Island .

617 The large, elongate Lomonosov Ridge microcontinent separated from the Barents-Kara margin as
618 the Eurasia Basin initiated, probably in part exploiting parallel fractures from the Amerasia Basin
619 terminal transform zone. Eurasia Basin spreading terminated at the Laptev margin, where extension
620 was partitioned between the Laptev Rift (Drachev et al., 1998) and strike-slip: westwards into the
621 Yenisey-Khatanga Trough and eastwards as renewed right-lateral movement along the Eastern
622 Siberian margin and into the Bering Strait (Figure 17).

623 Isochron 13 (33 Ma) marked a significant plate reorganization in the NE Atlantic and Arctic (Figure
624 18). Seafloor spreading terminated in the Labrador Sea and Baffin Bay (Kristoffersen & Talwani
625 1977). Consequently Greenland again became part of the North American plate, and the seafloor
626 spreading became focused on a single spreading axis linking the NE Atlantic and Eurasia Basin.
627 Greenland was therefore no longer forced northward and the Eurekan Orogeny terminated, as did the
628 West Spitsbergen Orogeny. The spreading vector between Greenland and Eurasia changed by c. 30°,
629 causing oblique opening of the pre-existing De Geer shear margin, release and outward drift of
630 microcontinental shards (Hovgaard and East Greenland Ridges), inception of the Knipovich
631 spreading ridge and passive drift between NE Greenland and the Barents Sea.

632 The Arctic gateway in the Fram Strait (between Greenland and Spitsbergen) became breached at c.
633 17.5 Ma and allowed oceanic circulation to start between the Arctic Ocean and the Atlantic (e.g.
634 Jakobsson et al., 2007). Activity on the Khatanga-Bering Shear Zone may have diminished after this
635 reorganization, with extension refocusing on the Laptev Rift from the Middle Miocene onwards
636 (Drachev et al., 1998).

637

638 **Implications for future Arctic work**

639 Most models for Cretaceous-Cenozoic Arctic evolution, and especially the 3-stage model proposed
640 above, imply that much of the oceanic area is bracketed by paleo-transform margins, and/or by
641 transforms that have been reactivated as passive margins. This observation makes definite and
642 testable predictions about geometries and basin modelling characteristics that will be encountered as
643 more data becomes available in the lesser-known Arctic areas. Transform margins have unique
644 geometries, distinct from those of rifted or active margins, and these structures have been studied in
645 some detail on the Atlantic equatorial transform zone (e.g. Mascle et al., 1995, Nemcok et al. 2012).
646 A similar array of structures has already been documented in parts of the Arctic, and should become
647 further evident as more data is gathered.

648 Timing of continental break-up in shear margins is ambiguous, and depends on whether it is defined
649 by passing of a given point on the continent by the spreading ridge, or by the time when already-
650 formed oceanic crust passes by the margin. The ocean forms without much preceding extension, by
651 lateral motion of one plate past the other, so margins tend to be expressed by an abrupt termination
652 of normal or moderately thinned continental crust against oceanic crust. Abrupt terminations of this
653 type are typical of parts of the Barents Sea western margin, for example along the Svalbard margin
654 (e.g. Myhre & Thiede 1995) and on the western peripheries of the Sørvestnaget Basin and
655 Vestbakken Volcanic Province (e.g. Gabrielsen et al., 1990) (Figure 7). Similar geometries are also
656 evident on the few seismic profiles across the eastern Siberian margin, where Sekretov (2001)
657 characterizes the Late Cretaceous paleo-margin via a “passive-transform model” associated with
658 opening of the Makarov-Povodnikov Basin. His published lines show abutment of Late Cretaceous
659 reflectors against steeply rising basement, albeit now buried beneath thick continental slope deposits
660 of Cenozoic age (Figure 13). New, currently unpublished Russian seismic lines across the Laptev
661 and East Siberian margin either side of the Lomonosov Ridge show further evidence of steep
662 margins and strike-slip deformation, including flower structures (A. Nikishin, Personal
663 Communication, 2015). We predict further confirmation of shear margin geometries along this little-
664 known margin as better seismic data sets are obtained, along with further expressions of small-scale
665 conjugate strike-slip fault assemblages of the type observed in the Hanna Trough, Alaska, described
666 above (c.f. Reches 1978; Krantz 1988).

667 Although on the grand scale transform margins appear to be long, straight features, in detail they
668 commonly consist of multiple parallel fractures, “horsetail” faulting and *en echelon* shear segments
669 (e.g. Mascle et al., 1995). Transpression and pull-apart occur at constraining or releasing bends or
670 between *the en echelon* segments, but also occur due to convergent or divergent motion across the
671 margin associated with plate reorganization and changes in the spreading vector. The Sørvestnaget
672 Basin and Vestbakken Volcanic Province are examples of Paleogene pull-apart basins at releasing
673 bends along the De Geer transform margin (Figures 6 & 7). Pull-part basins promote ridge-jump by
674 eventually developing spreading ridges in their axes (Nemcok et al. 2012), and this appears to have
675 taken place in the Vestbakken Volcanic Province, where the segmented margin steps eastwards and
676 the Eocene-Oligocene volcanism is probably associated with development of the ridge. It is worthy
677 of note that the De Geer margin has an intermittent igneous signature, which also includes
678 Quaternary volcanism documented on Spitsbergen (Treiman 2012). The association between
679 volcanism and ridge propagation in a transform margin setting – or, in some cases, the lack of it -
680 appears to have been little discussed in the literature (with a few exceptions, e.g. Mihut and Muller
681 1998) and is worthy of future investigation.

682 Changes in spreading vector on elements of the Equatorial Transform Margin such as the Romanche
683 and St Paul fracture zones, associated with the development of transpressive structures, appear to
684 have been in the order of 10-20 degrees (Nemcok et al. 2012). The De Geer shear margin, on the
685 other hand, has seen more radical changes in plate motion. These began in the Early Eocene with

686 the dextral shear occurring simultaneously with northwards convergence of Greenland with the
687 Barents and Arctic Canada margin. Simultaneously, sinistral shearing probably occurred along the
688 greater “Wegener fault” between Greenland and Ellesmere Island. The result was not just
689 transpressive uplift but the development of mountain ranges and full-scale fold-and- thrust belts in
690 Spitsbergen, North Greenland and Arctic Canada (Dallmann et al., 1993; Lyberis & Manby 1993).
691 Conversely, the c. 30 degree change in spreading direction at the Eocene-Oligocene transition
692 represented extreme divergence. This change resulted eventually in passive drift, although it is
693 notable that transtensional tectonics are still active today on the western margin of Spitsbergen
694 (Cianfarra & Salvini 2014). This area represents part of the De Geer Zone where the Knipovitch
695 Ridge has only just penetrated through the Fram Strait between Greenland and the Barents platform,
696 and where oblique ultra-slow spreading is taking place at present day (Snow et al., 2011) . The most
697 radical change in spreading vector in the Arctic occurred between the opening of the Canada and
698 Makarov-Povodnikov Basins. Here the change was almost 90 degrees, and in the view we have
699 promoted above this resulted in major shedding of microcontinental material from the former shear
700 margin during the late Cretaceous and Paleogene (see also Nemčok et al., this volume).

701 Transform margins have specific implications for basin modelling and thus for petroleum
702 exploration (e.g. Nemčok et al., 2012). Reservoir deposition is affected by steep slopes with low
703 sediment retention. Depositional fans are therefore likely to be separated from their shelf source
704 area. Entry points for clastic sediments tend to be focused at releasing bends with thickest deposits
705 in pull-apart basins. Because of the separation of source from depositional area by bypass,
706 stratigraphic traps become important, as exemplified by discoveries along the Equatorial Transform
707 Margin. In terms of thermal maturation history, modelling suggests that initial continental break-up
708 in a shear setting results in a warming event due to thinning of crust in pull-apart basins. This peak
709 is followed by cooling and then further warming as the spreading center passes along the margin
710 instead of moving away from it. This second heat flow maximum is reached during the passage time
711 of the spreading center. It is then followed again by cooling (see more detailed description of the
712 thermal modelling in Nemčok et al., 2012). In addition to thermal maturation, hydrocarbon
713 migration is also likely to be influenced by the margin type. Reactivation of strike-slip faults by
714 different stress regimes (strike-slip faulting, transtension, transpression), can occur long after initial
715 continental break-up. Therefore, fault-controlled hydrocarbon migration should be long-lasting and
716 variable during the post-rift history.

717 Thermally-induced uplift should also increase with the passing of the spreading ridge, but both this
718 type of uplift and uplift due to flexural unloading of the shear margin are exceeded by almost an
719 order of magnitude by transpressional effects (Clift & Lorenzo 1999, c.f. Nemčok et al., 2012).
720 Uplift and exhumation of a basin has radical, systematic effects on the petroleum system and
721 requires a different approach to exploration (Doré et al., 2002). Recent uplift of the margins appears
722 to be a pan-Arctic phenomenon, and, as might be expected, is most severe in the transpression-
723 compression dominated areas of the De Geer zone such as the north-western Barents Sea margin
724 (e.g. Henriksen et al., 2011) and Sverdrup Basin (e.g. Brooks et al. 1992).

725 The Equatorial and De Geer transform zones both represent globally-significant Atlantic transform
726 margins. Both are dextral and both are complex with multiple parallel components, but they differ
727 significantly in terms of plate kinematic evolution. These factors, plus the interest of the petroleum
728 industry in both areas, suggest that a more detailed future comparison of the two zones would pay
729 dividends in terms of understanding transform margin behaviour.

730

731 **Conclusions**

- 732 1. During the Cretaceous-Cenozoic opening history of the Arctic Ocean, transform margins existed
733 on three sides of the developing ocean. Transform margin development was a natural outcome of
734 opening around Euler poles in a relatively confined space, which is why all plate tectonic models for
735 the Arctic involve significant strike-slip motion. Timings and locations of the transform margins
736 were determined by spreading vectors, which changed radically during Arctic Ocean evolution.
- 737 2. A three-stage opening for the Arctic Ocean is argued to be the best kinematic fit and the most
738 reasonable correspondence with observed structural geometries and pre-opening volcanic episodes.
739 The model involves a Canada Basin rotational opening stage at 125-80 Ma, a Makarov-Podvodnikov
740 Basin stage (with Eurasian-Tethyan plate convergence) at 80-60 Ma orthogonal to the Canada Basin
741 spreading, and an adjacent, “mirror image” Eurasia Basin stage at 55-0 Ma. All of these opening
742 stages have been previously proposed in the literature, albeit not with this precise combination and
743 timing.
- 744 3. Canada Basin opening represents plate reorganization on the paleo-Pacific margin, specifically the
745 annealing of the South Anyui Sea, an embayment in the margin conceivably remaining from the
746 earlier (Late Paleozoic–early Mesozoic) Uralian closure. The radical change of break-up vector that
747 resulted in Makarov-Podvodnikov and Eurasia basin spreading represents a quite different influence
748 – northwards fragmentation of Pangea along the Atlantic trend. Makarov-Podvodnikov activity
749 appears to correspond with rifting and hyperextension in the Labrador Sea and Baffin Bay, while
750 Eurasia Basin spreading was synchronous with – and connected to – NE Atlantic activity.
- 751 4. The Grantz et al. (1979) rotational model still remains an excellent solution to early Amerasia
752 Basin opening, but we propose a modification such that the dextral terminal shear margin tracks the
753 arcuate Alpha-Mendeleev Ridge rather than the more linear Lomonosov Ridge. Volcanic dates on
754 and adjacent to the Alpha-Mendeleev Ridge are consistent with a separate opening of the Makarov-
755 Podvodnikov Basin, and this phase also provides a potential explanation for the widespread normal
756 faulting on the ridge. Further seismic data across the East Siberian Shelf, and palaeomagnetic data
757 documenting the rotation of the Chukotka/East Siberian shelf area, would help to pin down both the
758 existence and position of the Amerasia Basin Transform.
- 759 5. The De Geer line is a global-scale lineament that almost certainly began its existence as a Late
760 Paleozoic shear zone and was exploited during the separation of the Chukotka-Crocker Land terrane
761 from the Canadian Arctic margin in the Early Cretaceous. During the Cenozoic it formed a major
762 transform margin linking the Eurasia Basin and NE Atlantic, associated with transpression, pull-
763 apart and volcanism. The De Geer transform margin is strongly analogous to the similarly dextral
764 and extensive Equatorial shear margin, but experienced more radical changes in plate vector than the
765 latter. More detailed comparison of the two margins in terms of geometries, ridge-margin
766 interactions, volcanism and response to changing plate vectors would be fertile ground for future
767 study.
- 768 6. The existence of Late Cretaceous-Early Cenozoic shear along the Laptev-East Siberian
769 continental margin is highly likely as an outcome of, and accommodation to, Makarov-Podvodnikov
770 and Eurasia Basin opening. We have expressed this concept via the “Khatanga-Bering Transform”,
771 but readily accept that the shear may not be a single continuous feature. Although data is sparse in
772 this part of the Arctic, the available evidence is consistent with transform margin development,
773 including marginal geometries, lateral offsets and strike-slip fault assemblages. Transform motion
774 along the margin probably waned after the end-Eocene plate reorganization at Isochron 13 time, 33

775 Ma. While we predict that more evidence of shear will emerge as data coverage improves, work
776 should focus on two key factors; 1) further resolution of the amount of Cenozoic extension in the
777 Laptev Rift compared to the Eurasia Basin, and 2) evidence for transform margin and/or strike-slip
778 geometries on seismic lines across the Laptev margin, east Siberian margin, and within the Yenisey-
779 Khatanga Trough.

780 7. There appears to be an intimate connection between the Arctic transform margins and
781 microcontinent formation. Arctic microcontinents include the Hovgaard, East Greenland and
782 Lomonosov ridges and, we propose, continental material entrained in the Alpha-Mendeleev ridge.
783 In the Arctic, microcontinent escape appears to have taken place during, or as a result of, changes in
784 spreading vector. This connection appears to be a worldwide phenomenon and is considered in more
785 detail in a companion paper (Nemčok et al., this volume).

786 8. The sense of marginal transform motion in the Arctic appears to be overwhelmingly dextral, with
787 the possible exceptions of sinistral shear through the Yenisey-Khatanga Trough (Russia), Nares
788 Strait (Canada) and the theoretical (but unobserved) shear expressing the rotation of the Chukchi
789 Borderlands. The entire Atlantic also seems to be characterized by dextral offset on the major
790 transform margins, with the Arctic Ocean at the northern terminus of the system. This association
791 may be pure coincidence, or may represent a generic connection not yet understood.

792 9. The similar Equatorial and de Geer transform margins have both attracted petroleum industry
793 interest and include recent oil and gas discoveries. Recognition of a shear stage in the development
794 of a continental margin makes specific predictions on the petroleum system, including reservoir
795 deposition, traps, thermal history, migration, uplift and exhumation. Further detailed examination of
796 similarities and differences between the two transform zones could pay dividends both academically
797 and economically.

798

799 **References**

800 Alvey, A., Gaina, C., Kuszniir, N.J. & Torsvik, T.H. 2008. Integrated crustal thickness mapping and
801 plate reconstructions for the high Arctic. *Earth and Planetary Science Letters*, **274**, 310-321.

802

803 Amato, J.M., Toro, J., & Moore, T.E. 2004, Origin of the Bering Sea salient. *In: Sussman, A.J., &*
804 *Weil, A.B., eds., Orogenic curvature: Integrating paleomagnetic and structural analyses: Geological*
805 *Society of America Special Paper 383, 131–144.*

806 Balkwill, H.R. 1987. Labrador Basin: Structural and stratigraphic style. *In: Beaumont, C. &*
807 *Tankard, A.J. (eds.) Sedimentary Basins and Basin-Forming Mechanisms.* Canadian Society of
808 Petroleum Geologists Memoir, **12**, 17-43.

809 Bird, K.J. & Houseknecht, D.W. 2011. Geology and petroleum potential of the Arctic petroleum
810 province. *In: Spencer, A.M., Embry, A.F., Gautier, D.L., Stoupakova, A.V., and Sørensen, K., eds.,*
811 *Arctic Petroleum Geology: Geological Society, London, Memoirs, 35, 485-499.*

812 Boyden, J.A., Müller, R.D., Gurnis, M., Torsvik, T.H., Clark, J.A., Turner, M., Ivey-Law, H.,
813 Watson, R.J., & Cannon, J.S., 2011. *Next-generation plate-tectonic reconstructions using GPlates.*
814 *Geoinformatics: Cyberinfrastructure for the Solid Earth Sciences*, Keller G.R. & Baru, C., eds.,
815 Cambridge University Press, 2011.

- 816 Brooks, P.W., Embry, A., Goodarzi, F. & Stewart, R. 1992. Organic geochemistry and biological
817 marker geochemistry of Schei Point Group (Triassic) and recovered oils from the Sverdrup Basin
818 (Arctic Islands, Canada). *Bulletin of Canadian Petroleum Geology*, **40**, 173-187.
- 819 Brozena, J.M., Childers, V.A., Lawver, L.A., Gahagan, L.M., Forsberg, R., Faleide, J.I. & Eldholm,
820 O. 2003. New aerogeophysical study of the Eurasia Basin and Lomonosov Ridge: Implications for
821 basin development. *Geology*, **31**, 825-828.
- 822 Bruvoll, V., Kristoffersen, Y., Coakley, B.J., Hopper, J.R., Planke, S. & Kandilarov, A. 2012. The
823 nature of the acoustic basement on Mendeleev and northwestern Alpha ridges, Arctic Ocean.
824 *Tectonophysics*, **514**, 123-145, doi: DOI 10.1016/j.tecto.2011.10.015.
- 825 Carey, S.W. 1958. A tectonic approach to continental drift. In: Carey, S.W. (ed.) *Continental Drift:*
826 *A symposium*. Tasmania, Hobart, 177-355.
- 827 Churkin, M. & Trexler, J.H. 1980. Circum-Arctic Plate Accretion - Isolating Part of a Pacific Plate
828 to Form the Nucleus of the Arctic-Basin. *Earth and Planetary Science Letters*, **48**, 356-362, doi: Doi
829 10.1016/0012-821x(80)90199-5.
- 830 Cianfarra, P & Salvini, F. 2014. Lineament Domain of regional Strike-Slip Corridor: Insight from
831 the Neogene Transtensional De Geer Transform Fault in NW Spitsbergen. *Pure and Applied*
832 *Geophysics*. 17 pp. DOI: 10.1007/s00024-014-0869-9.
- 833 Clift, P. D. & Lorenzo, M. 1999. Flexural unloading and uplift along the Cote d'Ivoire Ghana
834 transform margin, Equatorial Atlantic. *Journal of Geophysical Research*, **104**, 25,257–25,274.
- 835 Colpron, M., Nelson, J.L. & Murphy, D.V. 2007. Northern Cordilleran terranes and their interactions
836 through time. *GSA Today*: **17**, 4/5, doi: 10.1130/GSAT01704-5A.1.
- 837 Corfu, F., Polteau, S., Planke, S., Faleide, J.I., Svensen, H., Zayoncheck, A. & Stolbov, N. 2013. U-
838 Pb geochronology of Cretaceous magmatism on Svalbard and Franz Josef Land, Barents Sea Large
839 Igneous Province. *Geological Magazine*, **150**, 1127-1135, doi: Doi 10.1017/S0016756813000162.
- 840 Dallmann, W.K., Andresen, A., Bergh, S.G., Maher jr., H.D. & Ohta, Y., 1993. Tertiary fold-and-
841 thrust belt of Spitsbergen Svalbard. Norsk Polarinstittutt, Meddelelser **128**, 46 pp.
- 842 Dixon, J. 1982. Jurassic and Lower Cretaceous subsurface stratigraphy of the Mackenzie Delta-
843 Tuktoyaktuk Penninsula. *Bulletin Canadian Geological Survey*, **349**, 52.
- 844 Doré, A.G., Corcoran, D.V. & Scotchman, I.C. 2002. Prediction of the hydrocarbon system in
845 exhumed basins, and application to the NW European margin. In Doré, A.G., Cartwright, J.A.,
846 Stoker, M.S., Turner, J.P. & White, N.J. 2002. *Exhumation of the North Atlantic Margin: Timing,*
847 *Mechanisms and Implications for Petroleum Exploration*. Geological Society, London, Special
848 Publications, **196**, 401-429
- 849 Drachev, S.S. 1998. Laptev Sea rifted continental margin: modern knowledge and unsolved
850 questions. *Polarforschung*, **68**, 41-50.
- 851 Drachev, S.S. 2011. Tectonic setting, structure and petroleum geology of the Siberian Arctic
852 offshore sedimentary basins. In: Spencer, A.M., Embry, A.F., Gautier, D.L., Stoupakova, A.V., and
853 Sørensen, K., eds., *Arctic Petroleum Geology*: Geological Society, London, Memoirs, **35**, 369-394.

- 854 Drachev, S.S., Kaul, N. & Beliaev, V.N. 2003. Eurasia spreading basin to Laptev Shelf transition:
855 structural pattern and heat flow. *Geophysical Journal International*, 152, 688-698, doi: DOI
856 10.1046/j.1365-246X.2003.01882.x.
- 857 Dutro, J.T. 1981. Geology of Alaska bordering the Arctic Ocean. In: Sweeney, J.F. (ed.) *Arctic*
858 *Geophysical Review*. Department of Energy Mines and Resources, Earth Physics Branch, Ottawa,
859 Canada, **45**, 87-90.
- 860 Døssing, A. & Funck, T. 2012. Greenland fracture Zone – East Greenland Ridge(s) revisited:
861 Indications of a C22-change in plate motion? *Journal of Geophysical Research*, 117, B01103,
862 doi:10.1029/2011JB008393, 22pp.
- 863
864 Døssing, A., Jackson, H.R., Matzka, J., Einarsson, I., Rasmussen, T.M., Olesen, A.V. & Brozena,
865 J.M. 2013. On the origin of the Amerasia Basin and the High Arctic Large Igneous Province-Results
866 of new aeromagnetic data. *Earth and Planetary Science Letters*, **363**, 219-230, doi: DOI
867 10.1016/j.epsl.2012.12.013.
- 868 Eldholm, O., Thiede, J. & Taylor, E. 1989. Evolution of the Voring volcanic margin margin. In:
869 Eldholm, O., et al. (ed.) *Proceedings of the Ocean Drilling Program, Norwegian Sea; covering Leg*
870 *104 of the cruises of the Drilling Vessel JOIDES Resolution, Bremerhaven, Germany, to St. John's,*
871 *Newfoundland, Sites 642-644, 19 June 1985-23 August 1985: College Station, Texas A & M*
872 *University, Ocean Drilling Program*, 1033-1065.
- 873 Faleide, J.I., Vågnes, E. & Gudlaugsson, S.T. 1993. Late Mesozoic-Cenozoic evolution of the
874 south-western Barents Sea in a regional rift-shear tectonic setting. *Marine and Petroleum Geology*,
875 10, 186-214.
- 876 Faleide, J.I., Bjørlykke, K. & Gabrielsen, R.H., 2010. Geology of the Norwegian Continental Shelf.
877 In: K. Bjørlykke (ed.), *Petroleum Geoscience: From Sedimentary Environments to Rock Physics*.
878 Springer Verlag Berlin, 508 pp.
- 879
880 Feden, R. H., Vogt, P. R. & Fleming, H. S. 1979. Magnetic and bathymetric evidence for the
881 'Yermak hot spot' northwest of Svalbard in the Arctic Basin. *Earth and Planetary Science Letters*,
882 **44**, 18-38.
- 883
884 Franke, D. & Hinz, K. 2005. The structural style of the sedimentary basins on the shelves of the
885 Laptev Sea and western East Siberian Sea, Siberian Arctic. *Journal of Petroleum Geology*, **28**, 269-
886 286.
- 887
888 Franke, D., Hinz, K. & Oncken, O. 2001. The Laptev Sea rift. *Marine and Petroleum Geology*, **18**,
889 1083-1127
- 890
891 Franke, D., Hinz, K. & Reichert, C. 2004. Geology of the East Siberian Sea, Russian Arctic, from
892 seismic images: structures, evolution, and implications for the evolution of the Arctic Ocean Basin.
893 *Journal of Geophysical Research-Solid Earth*, **109**, doi: Artn B07106. Doi 10.1029/2003jb002687.
- 894 Freund, R., Garfunkel, Z., Zak, I., Goldberg, M., Weissbrod, T. & Derin, B. 1970. The shear along
895 the Dead Sea rift. *Philosophical Transactions Royal Society (London) Series A*, **267**, 107-130.

- 896 Fujita, K., Cambray, F.W. & Velbel, M.A. 1990. Tectonics of the Laptev Sea and Moma Rift
897 Systems, Northeastern USSR. *Marine Geology*, 93, 95-118, doi: Doi 10.1016/0025-3227(90)90079-
898 Y.
- 899 Gabrielsen, R.H., Færseth, R.B., Jensen, L.N., Kalheim, J.E. & Riis, F. 1990. Structural elements of
900 the Norwegian continental shelf, Part 1: The Barents Sea Region. *NPD Bulletin*, 6, 47.
- 901 Gaina, C. & Werner, S.C. 2009. Circum-Arctic mapping project - gravity and magnetic maps
902 (CAMP-GM). *Norwegian Geological Survey (NGU) Report*, 21 pp.
- 903 Gaina, C., Roest, W.R. & Muller, R.D. 2002. Late Cretaceous-Cenozoic deformation of northeast
904 Asia. *Earth and Planetary Science Letters*, 197, 273-286, doi: Pii S0012-821x(02)00499-5. Doi
905 10.1016/S0012-821x(02)00499-5.
- 906 Gautier, D.L., Bird, K.J., Charpentier, R.R., Grantz, A., Houseknecht, D.W., Klett, T.R., Moore,
907 T.E., Pitman, J.K., Schenk, C.J., Schuenemeyer, J.H., Sørensen, K., Tennyson, M.E., Valin, Z.C.,
908 and CRAIG J. Wandrey, C.J. 2011. Oil and gas resource potential north of the Arctic Circle. In:
909 Spencer, A.M., et al. (eds.) *Arctic Petroleum Geology*. Geological Society, London, Memoirs, 35,
910 151-162.
- 911 Gee, D. G. & Teben'kov, A. M., 2004. Svalbard: a fragment of the Laurentian margin. Geological
912 Society, London, Memoir 30, 191-206.
- 913 Geissler, W.H., Jokat, W. & Brekke, H. 2011. The Yermak Plateau in the Arctic Ocean in the light
914 of reflection seismic data - implications for its tectonic and sedimentary evolution. *Geophysical*
915 *Journal International*, 187, 1334-1362.
- 916 Glen, J.M.G., 2004, A kinematic model for the southern Alaska orocline based on regional fault
917 patterns. In: Sussman, A.J., and Weil, A.B., (eds.), *Orogenic Curvature: Integrating Paleomagnetic*
918 *and Structural Analyses: Geological Society of America Special Paper 383*, 161-172.
- 919 Gogonenkov, G.N. & Timurziev, A.I. 2012. Strike-slip faulting in the West Siberian Platform:
920 Insights from 3D seismic imagery. *Comptes Rendus Geoscience*, 344, 214-226, doi: DOI
921 10.1016/j.crte.2011.09.010.
- 922 Golonka, J. 2011. Phanerozoic palaeoenvironment and palaeolithofacies maps of the Arctic region.
923 In: Spencer, A.M., Embry, A.F., Gautier, D.L., Stoupakova, A.V., and Sørensen, K., eds., *Arctic*
924 *Petroleum Geology: Geological Society, London, Memoirs*, 35, 79-129.
- 925 Grantz, A., Eittrheim, S. & Dinter, D.A. 1979. Geology and Tectonic Development of the
926 Continental-Margin North of Alaska. *Tectonophysics*, 59, 263-291, doi: Doi 10.1016/0040-
927 1951(79)90050-7
- 928 Grantz, A., Clark, D.L., Phillips, R.L., Srivastava, S.P., Blome, C.D., Gray, L.B., Haga, H., Mamet,
929 B.L., McIntyre, D.J., McNeil, D.H., Mickey, M.B., Mullen, M.W., Murchey, B.I., Ross, C.A.,
930 Stevens, C.H., Silberling, N.J., Wall, J.H. & Willard, D.A. 1998. Phanerozoic stratigraphy of
931 Northwind Ridge, magnetic anomalies in the Canada basin, and the geometry and timing of rifting in
932 the Amerasia basin, Arctic Ocean. *Geological Society of America Bulletin*, 110, 801-820, doi: Doi
933 10.1130/0016-7606(1998)110<0801:Psonrm>2.3.Co;2.

- 934 Grantz, A., Hart, P.E., and Childers, V.A., 2011, Geology and tectonic development of the Amerasia
935 and Canada Basins, Arctic Ocean. In: Spencer, A.M., Embry, A.F., Gautier, D.L., Stoupakova,
936 A.V., and Sørensen, K., eds., *Arctic Petroleum Geology*: Geological Society, London, Memoirs, 35,
937 771-799.
- 938 Halgedahl, S. & Jarrard, R. 1987. Paleomagnetism of the Kuparuk River formation from oriented
939 drill core: evidence for rotation of the Arctic Alaska plate. In: Tailleux, I. & Weimer, P. (eds.)
940 *Alaskan North Slope Geology, Pacific SEPM*, 2, 581-617.
- 941 Harrison, C.J. 2004. In search of the Wegener Fault: Re-evaluation of strike-slip displacements
942 along and bordering Nares Strait. *Polarforschung*, 74, 129-160.
- 943 Harrison, J.C. & Brent, T.A. 2011. Baffin Bay and its inverted rift system of Arctic eastern Canada:
944 stratigraphy, tectonics and petroleum potential. In: Spencer, A. M., Embry, A. F., Gautier, D. L.,
945 Stoupakova, A. V. & Sørensen, K. (eds): *Arctic Petroleum Geology*. Geological Society, London,
946 Memoirs, 35, 595-626.
- 947 Henriksen, E., Bjørnseth, H.M., Hals, T.K., Heide, T., Kiryukhina, T., Kløvjan, O.S., Larssen, G.B.,
948 Ryseth, A.E., Rønning, K., Sollid, K. & Stoupakova, A. 2011. Uplift and erosion of the greater
949 Barents Sea: impact on prospectivity and petroleum systems. In: Spencer, A. M., Embry, A. F.,
950 Gautier, D. L., Stoupakova, A. V. & Sørensen, K. (eds): *Arctic Petroleum Geology*. Geological
951 Society, London, Memoirs, 35, 271-281.
- 952 Houseknecht, D.W. & Bird, K.J. 2011. Geology and petroleum potential of the rifted margins of the
953 Canada Basin. In: Spencer, A.M., Embry, A.F., Gautier, D.L., Stoupakova, A.V., and Sørensen,
954 K., eds., *Arctic Petroleum Geology*: Geological Society, London, Memoirs, 35, 509-526.
- 955 Harland, W.B. 1965. The tectonic evolution of the Arctic-North Atlantic region, Royal Soc. London
956 Philos. Trans. 258, pp. 59-75.
- 957 Herron, E.M., Dewey, J.F. & Pitman, W.-C.I. 1974. Plate tectonic model for the evolution of the
958 Arctic. *Geology*, 377-380.
- 959 Jakobsson, M., Backman, J., Rudels, B., Nycander, J., Frank, M., Mayer, L., Jokat, W., Sangiorgi,
960 F., O'Regan, M., Brinkhuis, H., King, J. & Moran, K. 2007. The early Miocene onset of a ventilated
961 circulation regime in the Arctic Ocean. *Nature*, 447, 986-990, doi: Doi 10.1038/Nature05924.
- 962 Jakobsson, M., L. A. Mayer, B. Coakley, J. A. Dowdeswell, S. Forbes, B. Fridman, H. Hodnesdal,
963 R. Noormets, R. Pedersen, M. Rebecco, H.-W. Schenke, Y. Zarayskaya A, D. Accettella, A.
964 Armstrong, R. M. Anderson, P. Bienhoff, A. Camerlenghi, I. Church, M. Edwards, J. V. Gardner, J.
965 K. Hall, B. Hell, O. B. Hestvik, Y. Kristoffersen, C. Marcussen, R. Mohammad, D. Mosher, S. V.
966 Nghiem, M. T. Pedrosa, P. G. Travaglini, and P. Weatherall, The International Bathymetric Chart of
967 the Arctic Ocean (IBCAO) Version 3.0, Geophysical Research Letters, doi:
968 [10.1029/2012GL052219](https://doi.org/10.1029/2012GL052219).
- 969 Jokat, W. 2005, The sedimentary structure of the Lomonosov Ridge between 88°N and 80°N.
970 *Geophysical Journal International*, 163, 698–726.
- 971 Jokat, W., Geissner, W. & Voss, M. 2008. Basement structure of the north-western Yermak Plateau.
972 *Geophysical Research Letters*, 35, L05309, doi:10.1029/2007GL032892.

- 973 Jokat, W., Ickrath, M. & O'Connor, J. 2013. Seismic transect across the Lomonosov and Mendeleev
974 Ridges: Constraints on the geological evolution of the Amerasia Basin, Arctic Ocean. *Geophysical*
975 *Research Letters*, **40**, 5047-5051, doi: Doi: 10.1002/Grl.50975.
- 976 Jokat, W., Uenzelmann-Neben, G., Kristoffersen, Y. & Rasmussen, T. M. 1992. Lomonosov Ridge –
977 a double-sided continental margin. *Geology*, **20**, 887–890.
- 978 Kontorovich, A.E., Kontorovich, V.A., Ryzhkova, S.V., Shurygin, B.N., Vakulenko, L.G.,
979 Gaideburova, E.A., Danilova, V.P., Kazanenkov, V.A., Kim, N.S., Kostyreva, E.A., Moskvin, V.I.
980 & Yan, P.A. 2013. Jurassic paleogeography of the West Siberian sedimentary basin. *Russian*
981 *Geology and Geophysics*, **54**, 747-779, doi: DOI 10.1016/j.rgg.2013.07.002.
- 982 Krantz, R.W. 1988. Multiple Fault Sets and 3-Dimensional Strain - Theory and Application. *Journal*
983 *of Structural Geology*, **10**, 225-&, doi: Doi 10.1016/0191-8141(88)90056-9.
- 984 Kristoffersen, Y. & Talwani, M. 1977. Extinct Triple Junction South of Greenland and Tertiary
985 Motion of Greenland Relative to North-America. *Geological Society of America Bulletin*, **88**, 1037-
986 1049, doi: Doi 10.1130/0016-7606(1977) 88<1037:Etjsog>2.0.Co;2.
- 987 Kristoffersen, Y., Hall, J. K., Coakley, B., Hopper, J. and the Healy 2005 Seismic Team. 2008.
988 Extensive local seabed disturbance, erosion and mass wasting on Alpha Ridge, Central Arctic
989 Ocean: possible evidence for an extra-terrestrial impact? *Norwegian Journal of Geology*, **88**, 313-
990 320.
- 991 Kuzmichev, A.B. 2009. Where does the South Anyui suture go in the New Siberian Islands and
992 Laptev Sea? Implications for the Amerasia Basin origin. *Tectonophysics*, **463**, 86-108.
- 993 Larsen, H.C. & Saunders, A.D. 1998. Tectonism and volcanism at the southeast Greenland rifted
994 margin: A record of plume impact and later continental rupture. In: Saunders, A.D., et al. (ed.)
995 *Proceedings of the Ocean Drilling Program, Scientific Results*, **152**, 503-533.
- 996 Larsen, L.M., Heaman, L.M., Creaser, R.A., Duncan, R.A., Frei, R. & Hutchison, M. 2009.
997 Tectonomagmatic events during stretching and basin formation in the Labrador Sea and the Davis
998 Strait: evidence from age and composition of Mesozoic to Palaeogene dyke swarms in West
999 Greenland. *Journal of the Geological Society*, **166**, 999-1012, doi: Doi 10.1144/0016-76492009-038.
- 1000 Lawver, L.A., Grantz, A. & Gahagan, L.M. 2002. Plate kinematic evolution of the present Arctic
1001 region since the Ordovician. In: Miller, E.L., Grantz, A. & Klemperer, S.L. (eds.) *Tectonic Evolution*
1002 *of the Bering Shelf-Chukchi Sea-Arctic Margin and Adjacent Landmasses*, Geological Society of
1003 America, Special Paper, **360**, 333-358.
- 1004 Lundin, E.R. & Doré, A.G. 2005. The fixity of the Iceland hotspot on the Mid-Atlantic Ridge:
1005 observational evidence, mechanisms and implications for Atlantic volcanic margins. In: Foulger,
1006 G.R., Natland, J.H., Presnall, D.C. & Anderson, D.L. (Eds.) *Plates, plumes and paradigms*.
1007 Geological Society of America Special Paper 388, 627-652.
- 1008 Lyberis, N. & Manby, G. 1993. The origin of the West Spitsbergen Fold Belt from geological
1009 constraints and plate kinematics: implications for the Arctic. *Tectonophysics*, **224**, 371-391.

- 1010 Mann, U., Knies, J., Chand, S., Jokat, W., Stein, R. & Zweigel, J. 2009. Evaluation and modelling of
1011 Tertiary source rocks in the central Arctic Ocean. *Marine and Petroleum Geology*, **26**, 1624-1639,
1012 doi: DOI 10.1016/j.marpetgeo.2009.01.008.
- 1013 Mascle, J., Basile, C., Pontoise, B. & Sage, F. 1995. The Côte d'Ivoire-Ghana transform margin: an
1014 example of an ocean–continent transform boundary. In: Banda, E., Talwani, M. & Thorne, M. (eds)
1015 *Rifted Ocean–Continent Boundaries*. NATO ASI Series. Kluwer, Dordrecht, 339–327.
- 1016 Michael, P.J., Langmuir, C.H., Dick, H.J.B., Snow, J.E., Goldstein, S.L., Graham, D.W., Lehnert,
1017 K., Kurras, G., Jokat, W., Muhe, R. & Edmonds, H.N. 2003. Magmatic and amagmatic seafloor
1018 generation at the ultraslow-spreading Gakkel ridge, Arctic Ocean. *Nature*, **423**, 956-U951, doi: Doi
1019 10.1038/Nature01704.
- 1020 Miller, E.L., Toro, J., Gehrels, G., Amato, J.M., Prokoviev, A., Tuchkova, M.I., Akinin, V.V.,
1021 Dumitru, T.A., Moore, T.E. & Cecile, M.P. 2006. New insights into Arctic paleogeography and
1022 tectonics from U-Pb detrital zircon geochronology. *Tectonics*, **25**, doi: Artn Tc3013. Doi
1023 10.1029/2005tc001830.
- 1024 Mihut, D., & Müller, R.D. 1998. Volcanic margin formation and Mesozoic rift propagators in the
1025 Cuvier Abyssal Plain off Western Australia. *Journal of Geophysical Research*, **103(B11)**, 27135–
1026 27149. doi:10.1029/97JB02672.
- 1027 Moore, T.E, Dumitru, T.A., Adams, K.E., Witebsky, S.N. and Harris, A.G. 2002. Origin of the
1028 Lisburne Hills-Herald Arch structural belt: stratigraphic, structural, and fission-track evidence from
1029 the Cape Lisburne area, northwestern Alaska. In: Miller, E.L., et al. (ed.) *Tectonic Evolution of the*
1030 *Bering Shelf - Chukchi Sea - Arctic Margin and Adjacent Landmasses*. Geological Society of
1031 America Special Papers, 77-109.
- 1032 Moran, K., Backman, J., Brinkhuis, H., Clemens, S.C., Cronin, T., Dickens, G.R., Eynaud, F.,
1033 Gattacceca, J., Jakobsson, M., Jordan, R.W., Kaminski, M., King, J., Koc, N., Krylov, A., Martinez,
1034 N., Matthiessen, J., McInroy, D., Moore, T.C., Onodera, J., O'Regan, M., Palike, H., Rea, B., Rio,
1035 D., Sakamoto, T., Smith, D.C., Stein, R., St John, K., Suto, I., Suzuki, N., Takahashi, K., Watanabe,
1036 M., Yamamoto, M., Farrell, J., Frank, M., Kubik, P., Jokat, W. & Kristoffersen, Y. 2006. The
1037 Cenozoic palaeoenvironment of the Arctic Ocean. *Nature*, **441**, 601-605, doi: Doi
1038 10.1038/Nature04800.
- 1039 Myhre, A. M. and Eldholm, O. 1988. The Western Svalbard Margin. *Marine and Petroleum*
1040 *Geology* **5**, 134–156.
- 1041 Myhre, A.M. & Thiede, J. 1995. 1. North Atlantic gateways. *Proceedings of the Ocean Drilling*
1042 *Program, Initial reports* **151**, 5-26.
- 1043 Nemčok, M., Henk, A., Allen, R., Sikora, P.J., and Stuart, C. 2012. Continental break-up along
1044 strike-slip fault zones: observations from the Equatorial Atlantic, In: Mohriak, W.U., Danforth, Al;
1045 Post, P. J., Brown, D. E., Tari, G. T., Nemčok, M., and Sinha, S.T., Eds., *Conjugate Divergent*
1046 *Margins*. Geological Society, London, Special Publication. **369**, 537-556, doi: 10.1144/SP369.8
- 1047 Nemčok, M., Sinha, S. T., Doré, A.G., Davison, I., Mascle, J. and Lundin, E.R. This Volume.
1048 Mechanisms of micro-continent release associated with transform margins during continental break-
1049 up; a review.

- 1050 Nikishin, A.M., Malyshev, M.A. and Petrov, E.I. 2014. *Geological structure and history of the*
1051 *Arctic Ocean*. Published by European Association of Geoscientists and Engineers (EAGE
1052 Publications), The Netherlands, ISBN 978-94-6282-188-0, 88 pp.
- 1053 Ohta, Y., Dallmeyer, R. D. & Peucat, J. J. 1989. Caledonian Terranes in Svalbard. *Geological*
1054 *Society of America Special Paper* 230.
- 1055 Patton, W.W. & TAILLEUR, I.L. 1977. Evidence in the Bering Strait region for differential movement
1056 between North America and Eurasia, *Geological Society of America Bulletin*, **88**, 1298-1304.
- 1057 Puchkov, V.N. 2009. The evolution of the Uralian orogeny. In: Murphy, J.B., et al. (ed.) *Ancient*
1058 *Orogens and Modern Analogues*. Geological Society, London, Special Publications, 161-195.
- 1059 Reches, Z. 1978. Analysis of Faulting in 3-Dimensional Strain Field. *Tectonophysics*, **47**, 109-129,
1060 doi: Doi 10.1016/0040-1951(78)90154-3.
- 1061 Ren, S., Faleide, J.I., Eldholm, O., Skogseid, J. & Gradstein, F. 2003. Late Cretaceous - Paleocene
1062 tectonic evolution of the NW Vøring Basin. *Marine and Petroleum Geology*, **20**, 177-206.
- 1063 Rowley, D.B & Lottes, A.K. 1988. Plate-kinematic reconstructions of the North Atlantic and Arctic:
1064 Late Jurassic to Recent. *Tectonophysics*, **155**, 73-120.
- 1065 Ryseth, A., Augustson, J.H., Charnock, M., Haugerud, O., Knutsen, S.-M., Midbøe, P.S., Opsal, J.G.
1066 & Sundsbø, G., 2003. Cenozoic stratigraphy and evolution of the Sørvestsnaget Basin, southwestern
1067 Barents Sea. *Norwegian Journal of Geology* **83**, 107-130.
- 1068 Saunders, A.D., Fitton, J.G., Kerr, A.C., Norry, M.J. & Kent, R.W. 1997. The North Atlantic
1069 Igneous Province. In: Mahoney, J.J. & Coffin, M.F. (eds.) *Large Igneous Provinces: Continental,*
1070 *Oceanic and Planetary*. Geophysical Monograph, American Geophysical Union, **100**, 45-93.
- 1071 Sekretov, S.B. 2001. Northwestern margin of the East Siberian Sea, Russian Arctic: seismic
1072 stratigraphy, structure of the sedimentary cover and some remarks on the tectonic history.
1073 *Tectonophysics*, **339**, 353, doi: Doi 10.1016/S0040-1951(01)00108-1.
- 1074 Shephard, G.E., Müller, R.D. & Seton, M. 2013. The tectonic evolution of the Arctic since Pangea
1075 breakup: Integrating constraints from surface geology and geophysics with mantle structure. *Earth-*
1076 *Science Reviews*, **124**, 148-183. doi:10.1016/j.earssci.2013.05.012.
- 1077 Smallwood, J.R & White, R.S. 2002. Ridge-plume interaction in the North Atlantic and its influence
1078 on continental breakup and seafloor spreading. In: Jolley, D.W & Bell, B.R. (eds.) *The North*
1079 *Atlantic Igneous province: Stratigraphy Tectonic, Volcanic and magmatic Processes*. Geological
1080 Society, London, Special Publications, **197**, 15-37.
- 1081 Snow, J. & H. Edmonds. 2007. Ultraslow Spreading Ridges: Rapid Paradigm Changes.
1082 *Oceanography Special Issue on Mid Ocean Ridges*. **20**, 1, 90-101.
1083
- 1084 Snow, J.E., Hellebrand, E., von der Handt, A., Nauret, F., Gao, Y., & Schencke, H.W. 2011. Oblique
1085 nonvolcanic seafloor spreading in Lena Trough, Arctic Ocean. *Geochemistry, Geophysics,*
1086 *Geosystems*. doi:10.1029/2011GC003768, 11pp.

- 1087 Sokolov, S.D., Bondarenko, G.Y., Layer, P.W. & Kravchenko-Berezhnoy, I.R. 2009. South Anyui
1088 suture: tectonoco-stratigraphy, deformations, and principal tectonic events. *Stephan Mueller Special*
1089 *Publication Series*, **4**, 201-221.
- 1090 Spencer, A.M., Embry, A.F., Gautier, D.L., Stoupakova, A.V. & Sørensen, K. (eds.) 2011. *Arctic*
1091 *Petroleum Geology*. Geological Society, London, Memoirs, 35.
- 1092 Steckler, M.S. & ten Brink, U.S. 1986. Lithospheric strength variations as a control on new plate
1093 boundaries: examples from the northern Red Sea region. *Earth and Planetary Science Letters*, **79**,
1094 120-132.
- 1095 Taylor, P.T., Kovacs, L.C., Vogt, P.R. & Johnson, G.L. 1981. Detailed aeromagnetic investigations
1096 of the Arctic Basin. *J. Geophys. Res.*, **86** (1981), pp. 6323–6333
- 1097 Toro, J., Gans, P.B., McLelland, W.C. & Dumitru, T.A. 2002. Deformation and exhumation of the
1098 Mount Igikpak region, central Brooks Range, Alaska. In: Miller, E.L., et al. (ed.) *Tectonic Evolution*
1099 *of the Bering Shelf - Chukchi Sea - Arctic Margin and Adjacent Landmasses*. Geological Society of
1100 America Special Paper, **360**, 111-132.
- 1101 Torsvik, T.H., Løvlie, R. & Sturt, B.A., 1985. Palaeomagnetic argument for a stationary Spitsbergen
1102 relative to the British Isles (Western Europe) since late Devonian and its bearing on North Atlantic
1103 reconstruction. *Earth and Planetary Science Letters*, **75**, 278-288.
1104
- 1105 Treiman, A.H. 2012. Eruption age of the Sverrefjellet volcano, Spitsbergen Island, Norway. *Polar*
1106 *Research 2012*, **31**, 17320, DOI: 10.3402/polar.v31i0.17320
- 1107 Verzhbitsky, V., Frantzen, E.M., Trommestad, K., Savostina, T., Little, A., Sokolov, S.D.,
1108 Tuchkova, M.I., Travis, T., Martyntsiva, O. & Ullnæss, M. 2008. New seismic data on the South and
1109 North Chukchi sedimentary basins and the Wrangel Arch and their significance for the geology of
1110 the Chukchi Sea shelf. Extended abstract, 7 pp, *EAGE*, St. Petersburg
1111 ([http://www.tgs.com/uploadedFiles/CorporateWebsite/Modules/Articles_and_Papers/Papers/new-](http://www.tgs.com/uploadedFiles/CorporateWebsite/Modules/Articles_and_Papers/Papers/new-seismic-data-on-the-south-and-north-chukchi-sedimentary.pdf)
1112 [seismic-data-on-the-south-and-north-chukchi-sedimentary.pdf](http://www.tgs.com/uploadedFiles/CorporateWebsite/Modules/Articles_and_Papers/Papers/new-seismic-data-on-the-south-and-north-chukchi-sedimentary.pdf)).
- 1113 Vernikovskiy, V.A., Dobretsov, N.L., Metelkin, D.V., Matushkin, N.Y. & Koulakov, I.Y. 2013a.
1114 Concerning tectonics and the tectonic evolution of the Arctic. *Russian Geology and Geophysics*, **54**,
1115 838-858, doi: DOI 10.1016/j.rgg.2013.07.006.
- 1116 Vernikovskiy, V.A., Metelkin, D.V., Tolmacheva, T.Y., Malyshev, N.A., Petrov, O.V., Sobolev,
1117 N.N. & Matushkin, N.Y. 2013b. Concerning the Issue of Paleotectonic Reconstructions of the Arctic
1118 and of the Tectonic Unity of the New Siberian Islands Terrane: New Paleomagnetic and
1119 Paleontological Data. *Doklady Earth Sciences*, **451**, 2, 791-797.
- 1120 Vyssotski, A.V., Vyssotski, V.N. & Nezhdanov, A.A. 2006. Evolution of the West Siberian Basin.
1121 *Marine and Petroleum Geology*, **23**, 93-126, doi: DOI 10.1016/j.marpetgeo.2005.03.002.
- 1122 Wienecke, S. Fichler, C., Lundin, E., Stadtler, C., & Gram, C. 2011. Satellite measurements and
1123 global datasets in the Arctic: the benefits of the ASEP method. Abstract, AAPG Arctic 3P
1124 Conference, Halifax, Aug 30-Sep 2, 2011.

1125 Williams, S.E., Müller, D.R., Landgrebe, T.C.W. & Whittaker, J.M. 2012, An open source software
1126 environment for visualizing and refining plate tectonic reconstructions using high-resolution
1127 geological and geophysical data sets: *GSA Today*, **22**, 4/5, doi:10.1130/GSATG139A.1.

1128 Worsley, D. & Aga, O.J. 1986. The Geological History of Svalbard. Published by Statoil,
1129 Stavanger, Norway.

1130

1131 Ziegler, P.A. 1988. Evolution of the Arctic-North Atlantic and the Western Tethys. *American*
1132 *Association of Petroleum Geologists Memoir* **43**, 198 pp.

1133

1134

1135

1136

1137

1138

1139

1140

1141

1142

1143

1144

1145

1146

1147

1148

1149

1150

1151

1152

1153

1154

1155

1156

1157

1158

1159

1160

1161

1162 **Figure Captions**

1163

1164

1165 **Figure 1**

1166

1167 Bathymetry-topography map showing general physiographic elements of the Arctic.

1168

1169 **Figure 2**

1170

1171 Tectonic elements map of the Arctic. AB = Anabarsky Block, BAB = Baffin Bay, BB = Bjørnøya
1172 Basin, BI = Banks Island, BR = Brooks Range, BS = Baltic Shield, CAO = Caledonian Orogen, CB
1173 = Canada Basin, CFB = Coleville foreland basin, CO = Chukotka Orogen, DLH = De Long High,

1174 EBMB = Eastern Barents Megabasin, EO = Eureka Orogen, FJL = Franz Josef Land, GFZ =
1175 Greenland Fracture Zone, HAB = Hammerfest Basin, HB = Hope Basin, HR = Hovgaard Ridge, HT
1176 = Hanna Trough, JM = Jan Mayen, KBS = Khatanga-Bering Transform, LH = Laptev Horst, LR =
1177 Laptev Rift, LSB = Long Strait Basin, MD = Mackenzie Delta, MJR = Morris Jessup Rise, MR =
1178 Mendeleev Ridge, NCB = North Chukchi Basin, NGS = Norwegian-Greenland Sea, NKB =
1179 Nordkapp Basin, NKS = North Kara Sea, NS = Nares Strait, SAS = South Anyui Suture, SB =
1180 Sverdrup Basin, SH = Stappen High, SKS = South Kara Sea, SV = Svalbard, TB = Thetis Basin,
1181 TFB = Taimyr Foldbelt, TRB = Tromsø Basin, VFB = Verkhoyansk Foldbelt, WI = Wrangel Island,
1182 WS = West Siberia Basin, YKT = Yenisey-Khatanga Trough, YP = Yermak Plateau.

1183

Figure 3

1184

1185

1186 Crustal thickness map to show main crustal elements of the Arctic. Potential continent-ocean
1187 boundaries are indicated by dotted lines. AR = Alpha Ridge, BB = Baffin Bay, CB = Canada Basin,
1188 EB = Eurasia Basin, LR = Lomonosov Ridge, MPB = Makarov-Podvodnikov Basin, MR =
1189 Mendeleev Ridge, NEA = Northeast Atlantic. The crustal thickness, supplied by A. Alvey, was
1190 inverted from gravity data according to techniques described in Alvey et al., (2008). Image courtesy
1191 Badley Geoscience Ltd and OCTek.

1192

Figure 4

1193

1194

1195 Bouger gravity map of the Arctic (from Gaina & Werner 2009) showing the proposed locations of
1196 principal shears. ABT = Amerasia Basin Transform, CBT = Chukchi Borderlands Transform, DGL
1197 = De Geer Line, EJMFZ = East Jan Mayen Fracture Zone, HT = Hanna Transform, UFZ = Ungava
1198 Fracture Zone, 64FZ = 64 Degree West Fracture Zone = WHA = Wrangel-Herald Arch, WJMFZ =
1199 West Jan Mayen Fracture Zone.

1200

Figure 5

1201

1202

1203 Principal basement domains of the Barents Sea area, showing probable late Paleozoic expression of
1204 the De Geer Line. Adapted from Gee & Teben'kov (2004).

1205

Figure 6

1206

1207

1208 Break-up and evolution of the western Barents Sea (De Geer) shear margin, adapted from Faleide et
1209 al. (2010) and others. Abbreviations: AR = Aegir Ridge, BB = Bjørnøya Basin, EFB = Eureka Fold
1210 Belt, EGR = East Greenland Ridge, HAB = Harstad Basin, HR = Hovgaard Ridge, JM = Jan Mayen
1211 Microcontinent, JMFZ = Jan Mayen Fracture Zone, KNR = Knipovitch Ridge, KR = Kolbeinsey
1212 Ridge, MJR = Morris-Jessup Rise, MR = Mohn's Ridge, NR = Nansen-Gakkel Ridge, SVB =
1213 Sørvestnaget Basin, TB = Tromsø Basin, THB = Thetis Basin, VOB = Vøring Basin, VVP =
1214 Vestbakken Volcanic Province, WSFB = West Spitsbergen Fold and Thrust Belt, YP = Yermak
1215 Plateau.

1216

Figure 7

1217

1218

1219 Paleogene tectonic reconstruction of the western Barents Sea (De Geer) shear margin with seismic
1220 sections. The map is a composite for the Paleogene drawn on a 40 Ma (Eocene) base map. It does
1221 not indicate a precise time, but is designed to show the interrelationship between the shear margin,
1222 spreading cells, pull-apart basins and fold belts. Section A-A' is across the Vestbakken Volcanic
1223 Province, from TGS survey NPD-BJV2-86R05, courtesy TGS. Section B-B' is across the
1224 Sørvestnaget Basin. Abbreviations: BB = Bjørnøya basin, BFZ = Billefjorden Fault Zone, GFZ =

1225 Greenland Fracture Zone, H = Hovgaard Ridge, L = Lomonosov Ridge, LH = Loppa High, OCT =
1226 Ocean-Continent Transition, SCB = Spitsbergen Central Basin, SFZ = Senja Fracture Zone, SH =
1227 Stappen High, SVB = Sørvestnaget Basin, VVP = Vestbakken Volcanic Province, WSFB = West
1228 Spitsbergen Fold and Thrust Belt, YP = Yermak Plateau.

1229

1230 **Figure 8**

1231

1232 Sketch maps showing potential tracks of the proposed Amerasia Basin rotational shear. Upper map:
1233 general relationship of the alternative shear tracks to the Canada Basin extinct spreading ridge and
1234 pole of rotation in the Mackenzie Delta. Lower map: generalized geological units of the Siberian
1235 margin showing relationship to New Siberian Islands, fold belts and terranes. AR = Alpha Ridge, B
1236 = Barents Sea, CBL = Chukchi Borderlands, ER = Extinct spreading ridge of the Canada Basin, ES
1237 = East Siberian shelf, G = Greenland, LR = Lomonosov Ridge, MD = Mackenzie Delta, MJR =
1238 Morris-Jessup Rise, MR = Mendeleev Ridge, NSA = North Slope of Alaska, NSB = New Siberian
1239 Basin, NSI = New Siberian Islands, SB = Sverdrup Basin, YP = Yermak Plateau.

1240

1241 **Figure 9**

1242

1243 Maps pertaining to the discussion on shear along the Siberian margin. a) Bouger gravity map (from
1244 Gaina & Werner 2009). b) Structural features. Abbreviations: AB = Anisin Basin; ABT = Amerasia
1245 Basin Transform; AR = Alpha Ridge, CBT = Chukchi Borderlands transform; ChP = Chukchi
1246 Plateau, COB = Continental-ocean boundary; Cz = Cenozoic; DF = Denali Fault ; ESB = East
1247 Siberian Basin; HB= Hope Basin; HT = Hanna Transform; INFF = Idatarod-Nixon Fork Fault; KaF
1248 = Kaltag Fault, KBT = Khatanga-Bering transform, KoF = Kobuk Fault, KuF = Kugruk Fault, LSB
1249 = Long Strait Basin; MR = Mendeleev Ridge, NCB = North Chukchi Basin; NSB = New Siberian
1250 Basin; SAS= South Anyui Suture; SCB = South Chukchi Basin; TF = Tintina Fault; ULR = Ust-
1251 Lena Rift; WHA = Wrangel-Herald Arch; WI = Wrangel Island.

1252 **Figure 10**

1253

1254 Birdseye view of bathymetric-topographic map of the Eurasia Basin viewed from the Norway-
1255 Greenland side, illustrating termination against the Laptev shelf. Based on IBCAO map (Jakobsson
1256 et al.)

1257

1258 **Figure 11**

1259

1260 NE-SW crustal profile across Western Laptev Rift, the most extended part of the rift (from Franke et
1261 al. 2001). Note that the remaining crust is in the order of 10 km thick even where thinnest. A direct
1262 continuation of the Eurasia Basin into the Laptev Rift would require the continental crust to
1263 essentially be absent. Profile location is shown on Figure 9b.

1264

1265 **Figure 12**

1266

1267 Satellite image showing the termination of Red Sea spreading against the sinistral Dead Sea
1268 Transform, a suggested analogy for the termination of the Eurasia Basin against the Laptev Rift.

1269

1270 **Figure 13**

1271

1272 North-south profile (after Sekretov 2001) across the East Siberian continental margin. Note steep
1273 Cretaceous margin and candidate position of the Khatanga-Bering Transform at the site of
1274 substantial offset and pinch-out of the Cretaceous succession. Profile location is shown on Figure 9b.

1275
1276
1277
1278
1279
1280
1281
1282
1283
1284
1285
1286
1287
1288
1289
1290
1291
1292
1293
1294
1295
1296
1297
1298
1299
1300
1301
1302
1303
1304
1305
1306
1307
1308
1309
1310
1311
1312
1313
1314
1315
1316
1317
1318
1319
1320
1321
1322

Figure 14

Atlantic Ocean map showing series of transform faults and paleo-shear margins separating oceanic segments of differing ages and terminating at the proposed Khatanga-Bering Transform (KBT). AG = Azores-Gibraltar Fracture Zone, CG = Charlie Gibbs Fracture Zone, DGL = De Geer Line, E = Equatorial Shear Zone, F = Florianopolis Fracture Zone, FA = Falklands Fracture Zone.

Figure 15

Present day (0 Ma) plate tectonic setting and model. Abbreviations: AR = Alpha Ridge, CB = Chukchi Borderlands, JM = Jan Mayen Microcontinent, MPB = Makarov-Podvodnikov Basin, MR = Mendeleev Ridge, SAS = South Anyui suture, WI = Wrangel Island, WS = West Spitsbergen orogen.

Figure 16

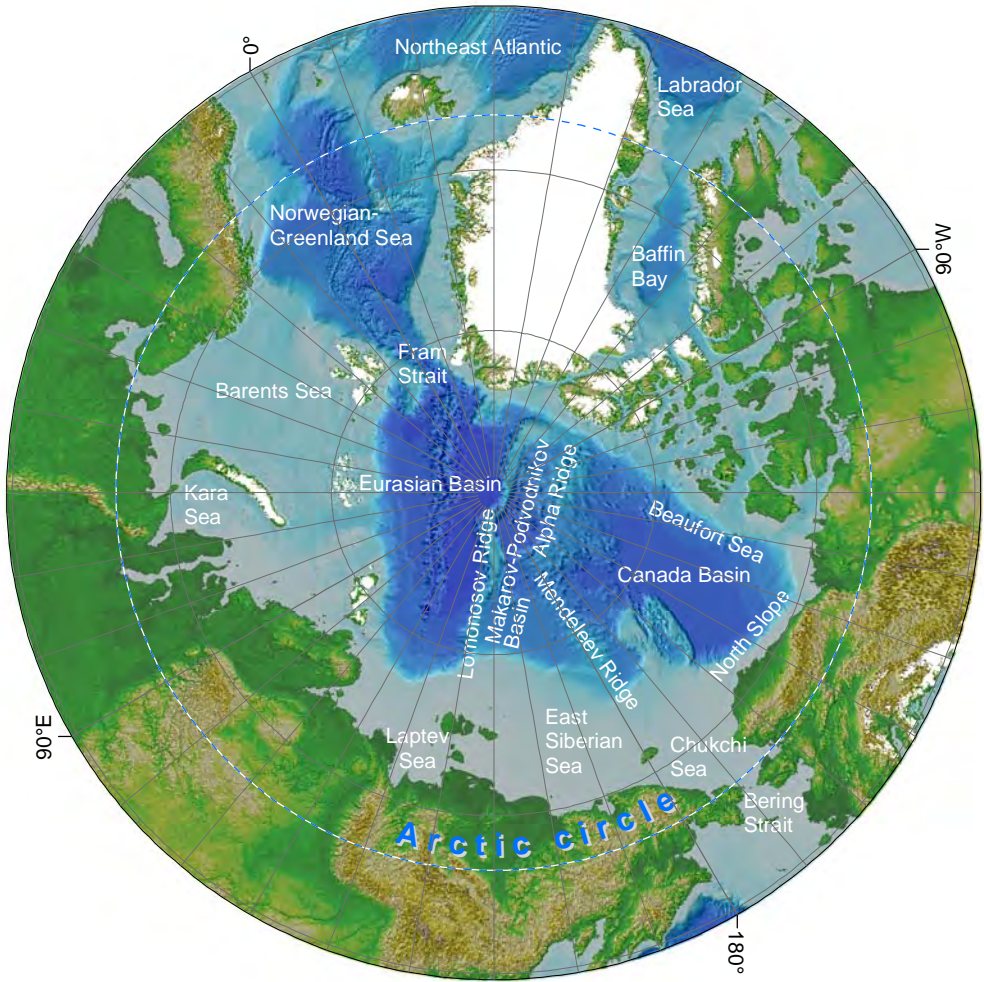
Plate reconstructions at 125 and 100 Ma. For legend see Figure 15. Abbreviations: BR = Brooks Range; CAB = Canada Basin; CB = Chukchi Borderlands; NAC = North America Cordillera; SAS = South Anyui Sea; WI = Wrangel Island

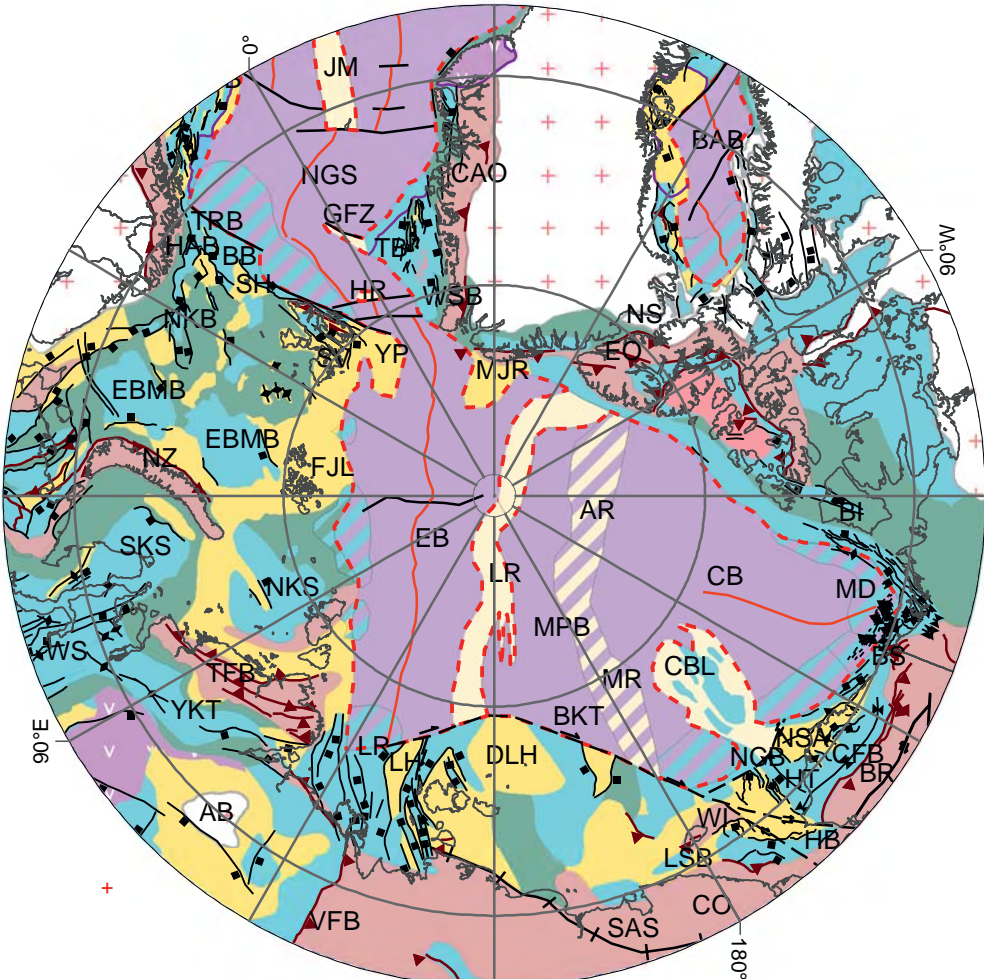
Figure 17

Plate reconstructions at 80 and 60 Ma. For legend see Figure 15. Abbreviations: AMR = Alpha-Mendeleev Ridge; BB = Baffin Bay; LS = Labrador Sea; MPB = Makarov-Podvodnikov Basin

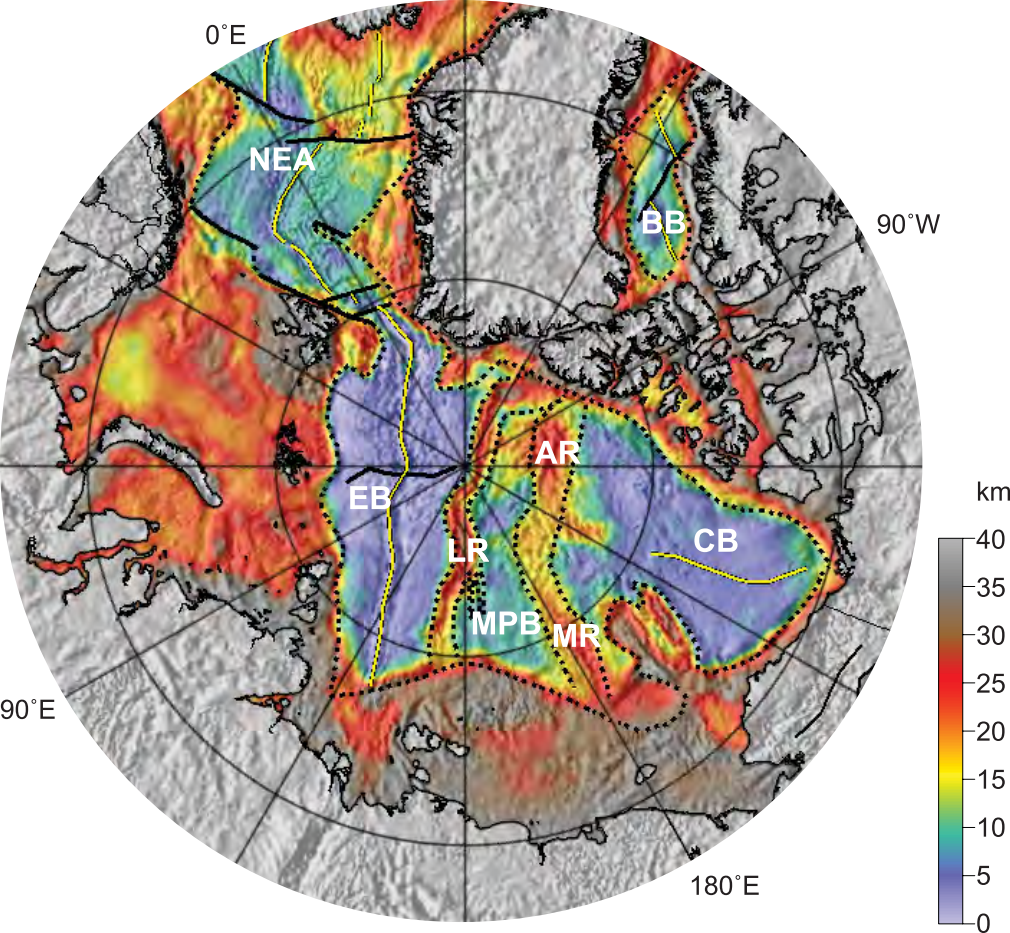
Figure 18

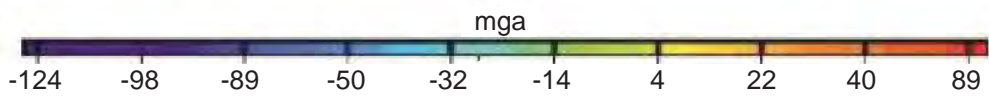
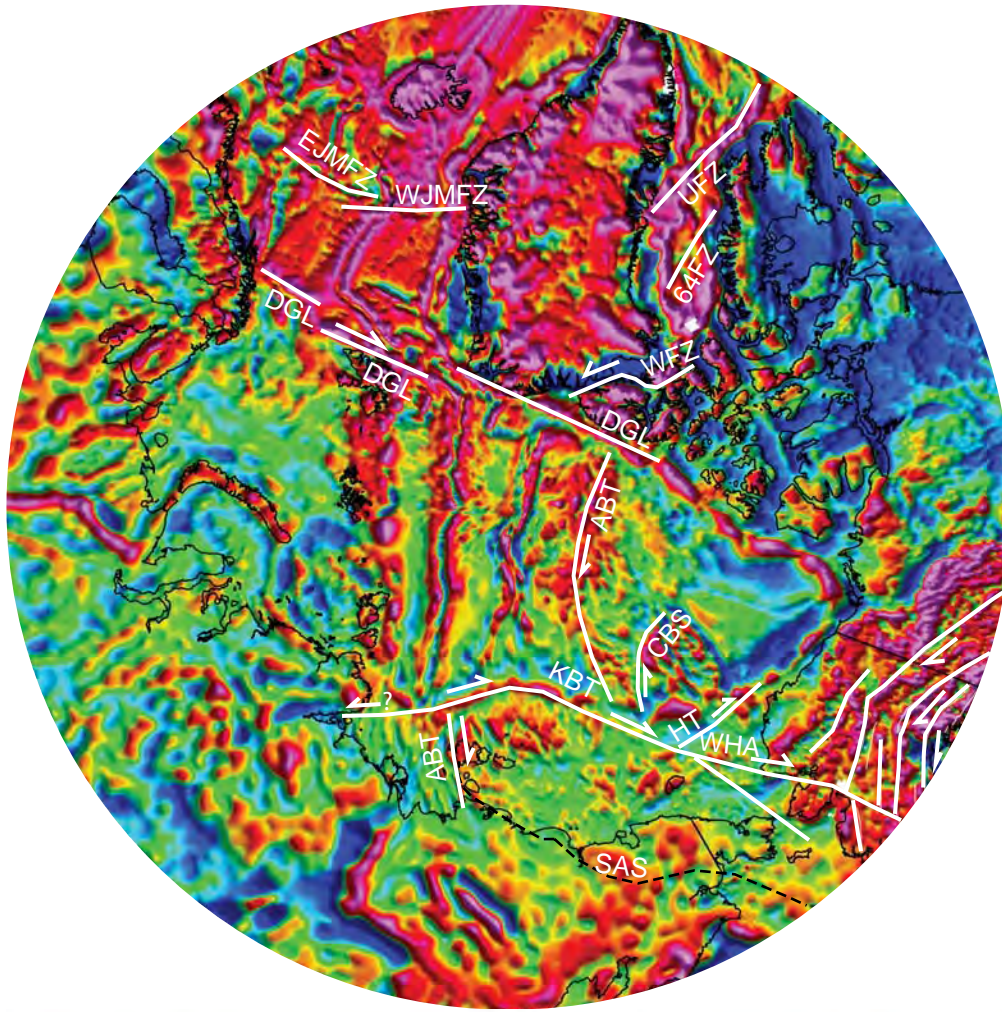
Plate reconstruction at 33 Ma. For legend see Figure 15. Abbreviations: BB = Baffin Bay; LS = Labrador Sea; SV = Svalbard

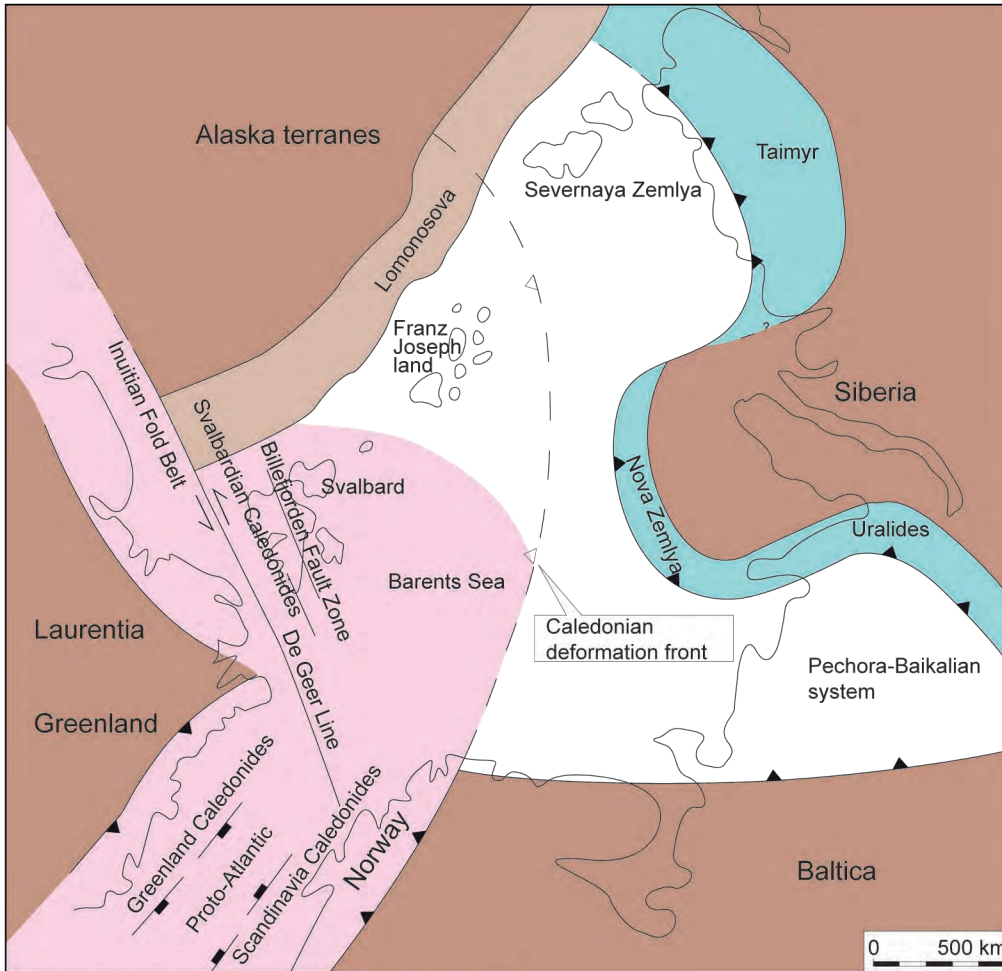




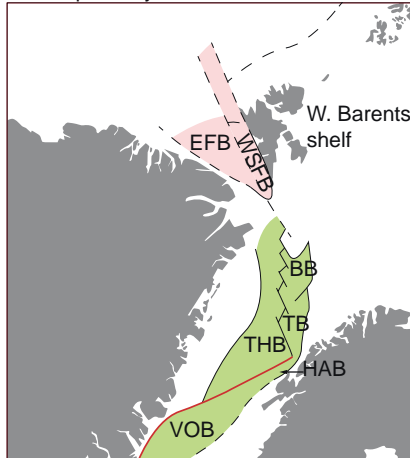
- | | | |
|------------------|--------------------------|--------------------|
| High | Volcanic | Syncline |
| Basin | Major fans | Fracture zone |
| Terrace/platform | Craton | Spreading axis |
| Microcontinent | Continent ocean boundary | Shear zone |
| Triassic rifts | Thrust | Volcanic |
| Oceanic crust | Extensional fault | South Anyui Suture |
| Orogen/foldbelt | Anticline | |



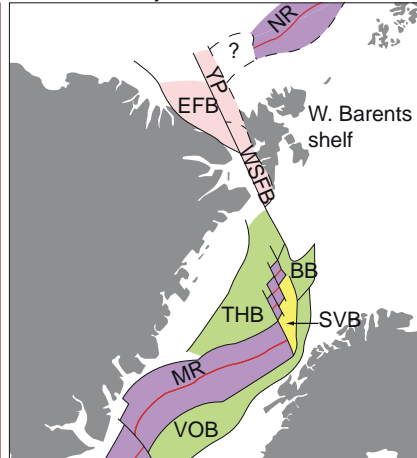




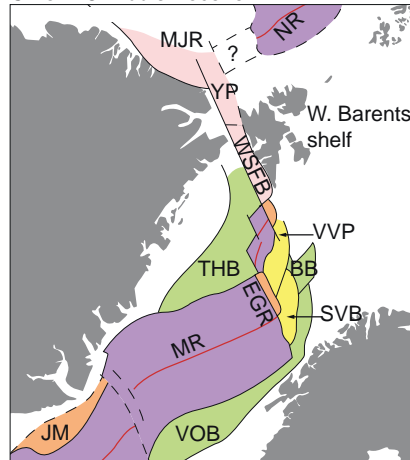
Breakup - Early Eocene



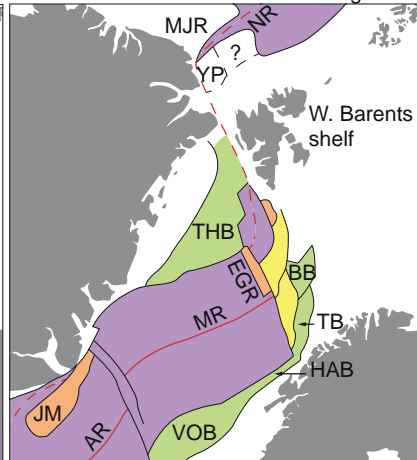
Chron 22 - Early Eocene



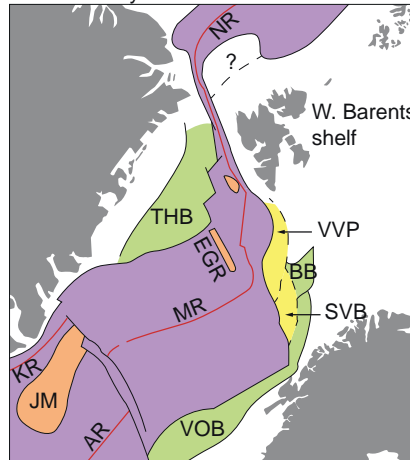
Chron 18 Middle Eocene



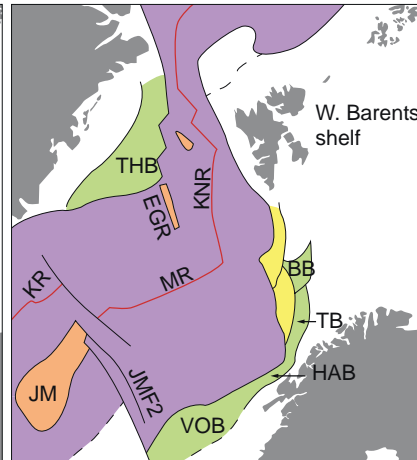
Chron 13 Latest Eocene-Earliest Oligocene



Chron 6 Early Miocene



Present



— Ocean floor

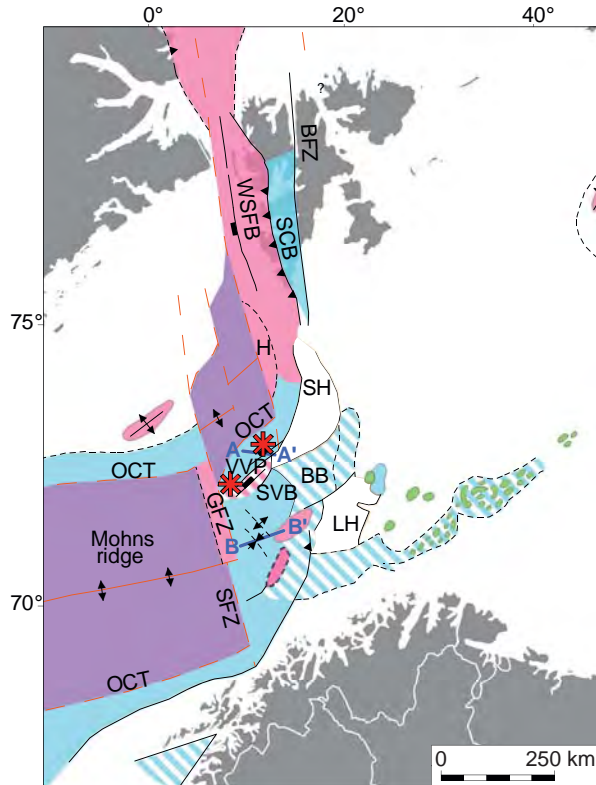
— Micro continent

— Orogen

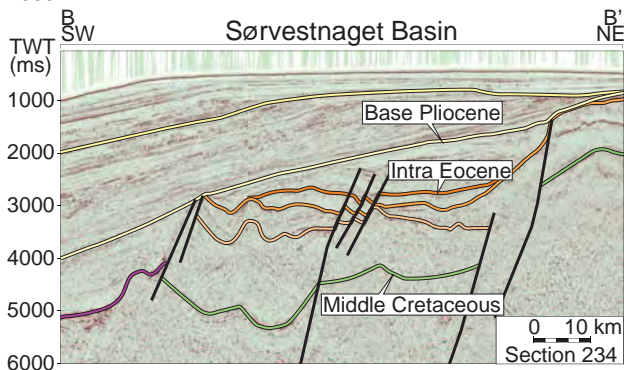
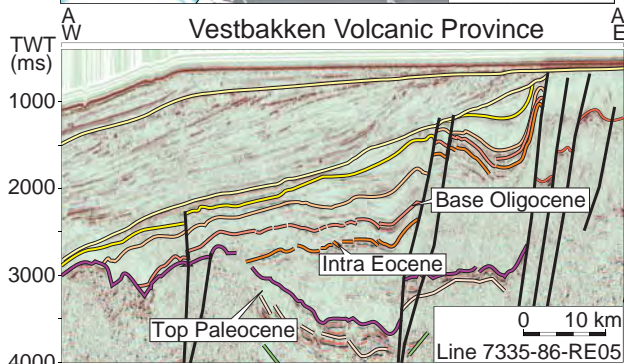
— Cenozoic basin

— Cretaceous basin

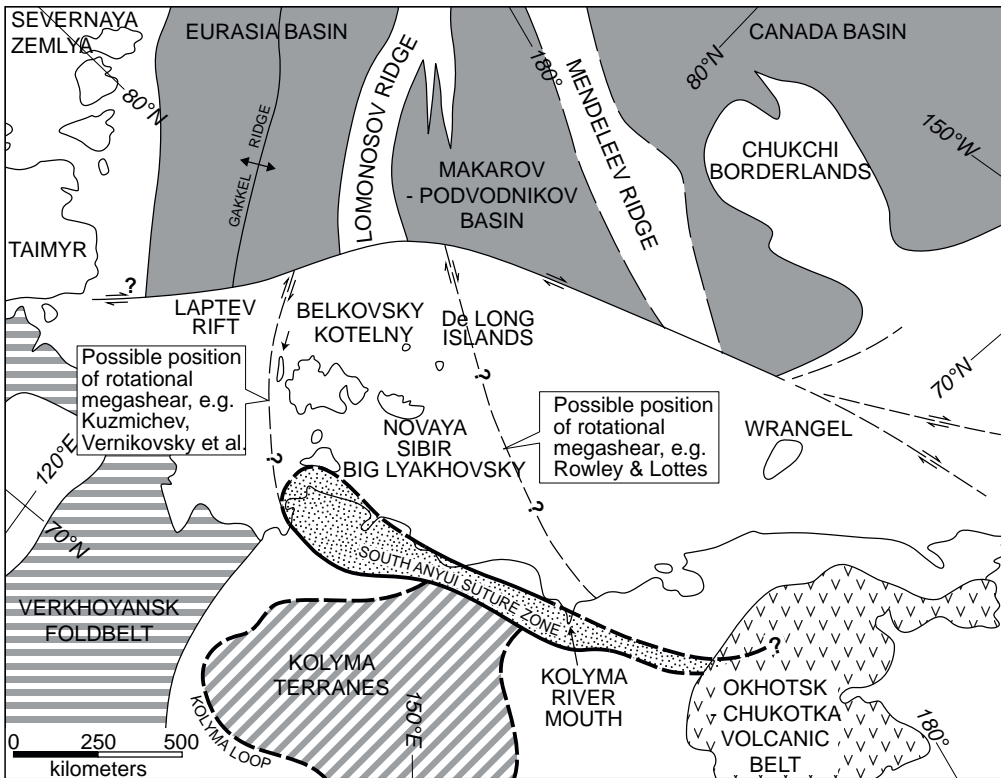
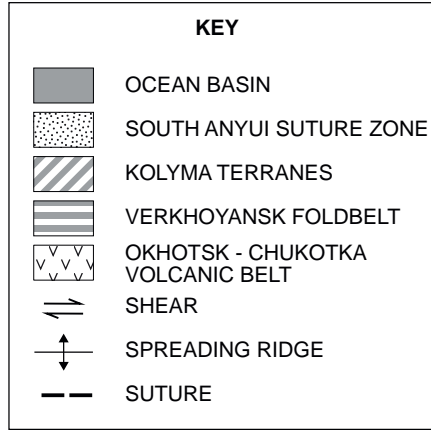
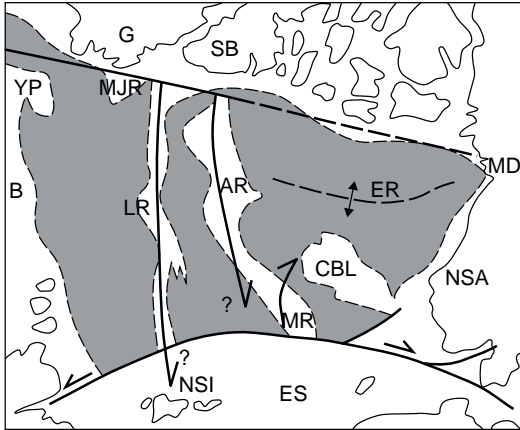
— Active or incipient spreading ridge

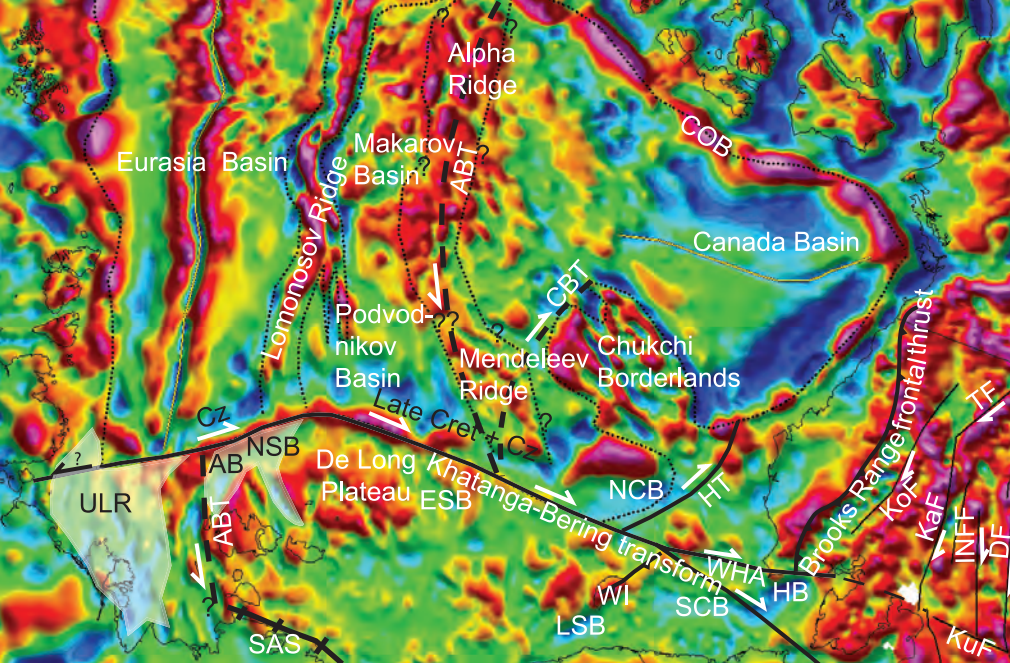


- Present land
- Extensional basin
- Ocean floor
- Halokinetic activity
- Compression/Inversion
- Possible/transient compr/inversion
- Possible/transient extensional basin
- Approx line of Paleogene break-up
- - - Lineament
- Min/maj normal faulting
- ▼ Known deformation front
- ★ Volcanism
- ⊥ Anticline
- ⊥ Syncline
- Profile

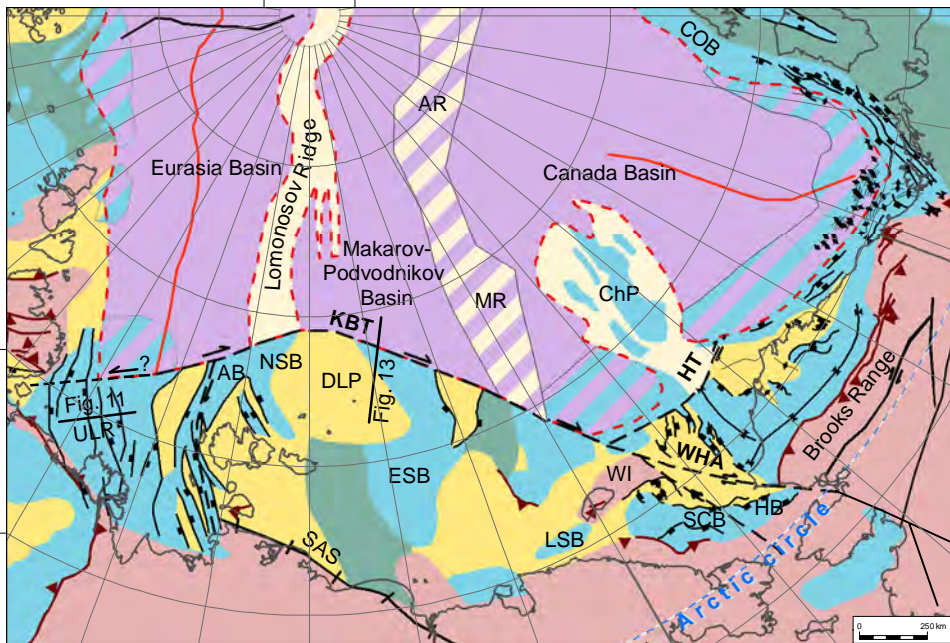


- Base Quaternary
- Base Pliocene
- Intra Miocene
- Intra Oligocene
- Base Oligocene
- Intra Eocene
- Top Volcanics
- Top Paleocene
- Intra Upper Paleocene
- Middle Cretaceous
- Top Basement

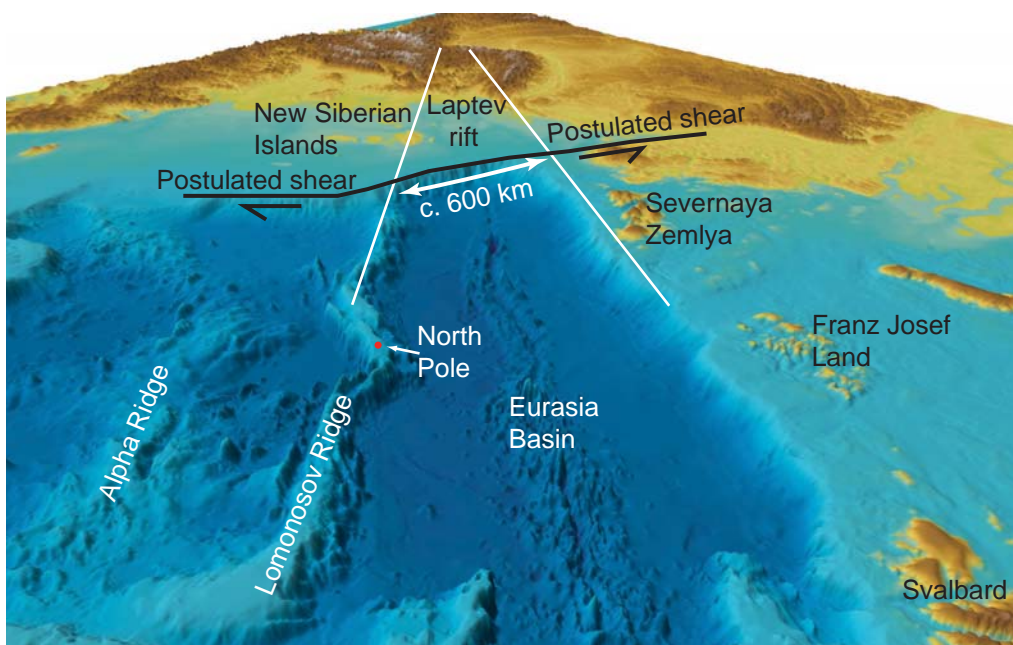


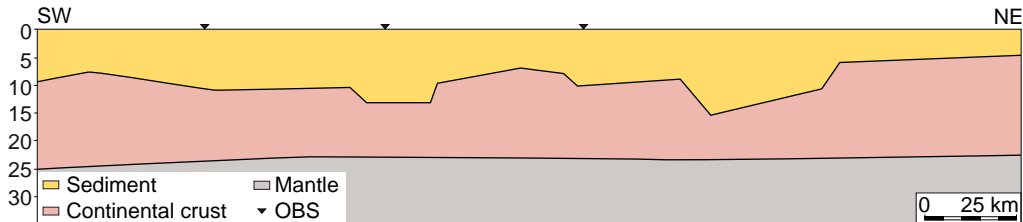
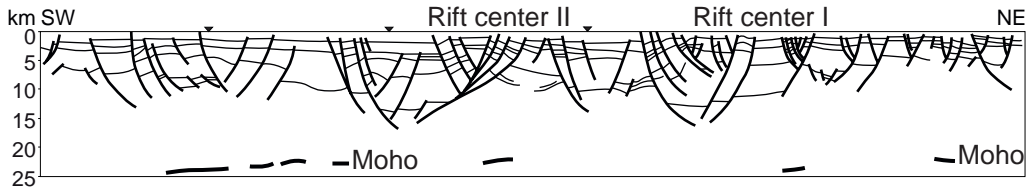


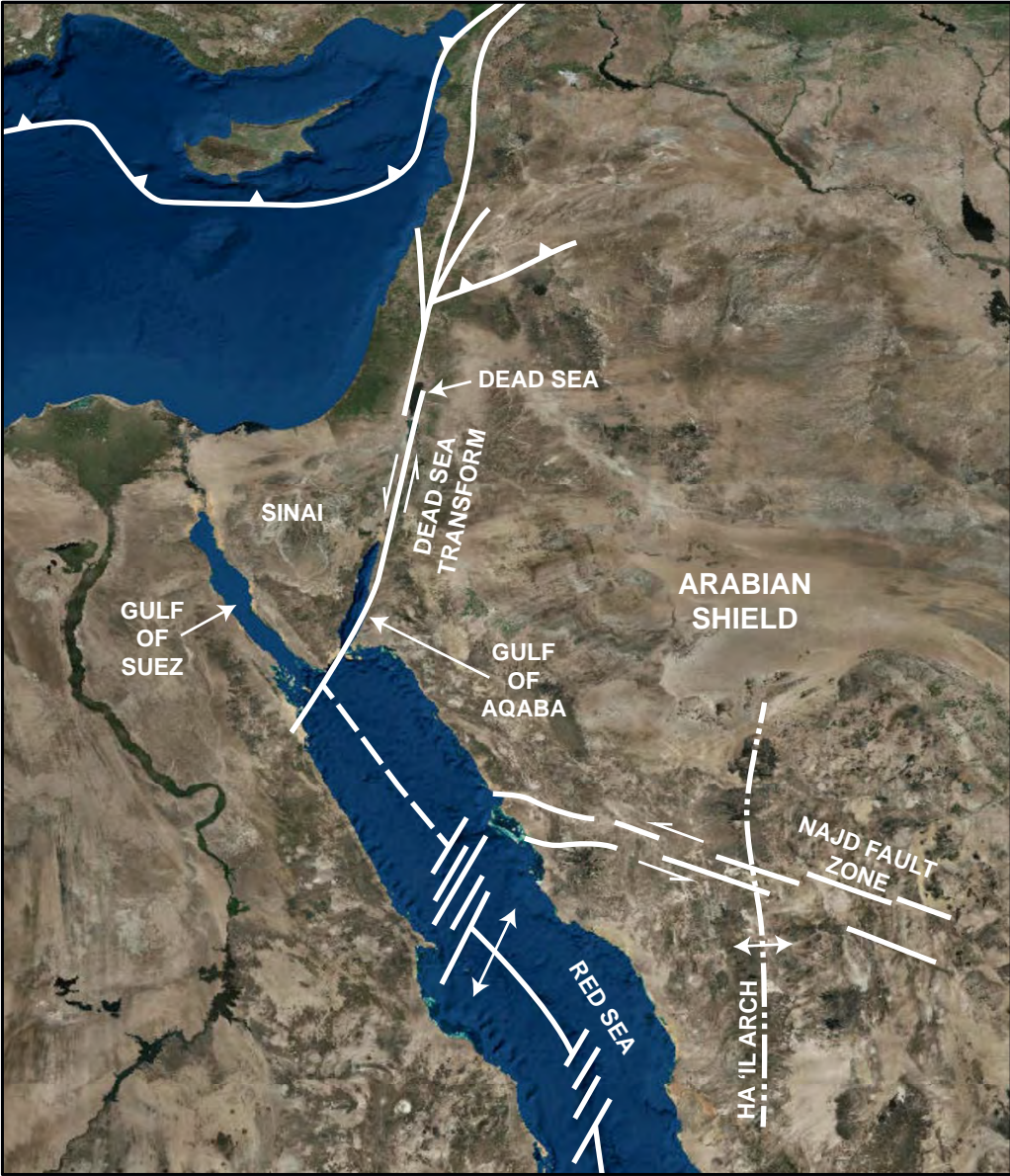
50°E 110°W



- | | | |
|------------------|--------------------------|----------------|
| High | Major fans | Syncline |
| Basin | Continent ocean boundary | Fracture zone |
| Terrace/platform | Thrust | Spreading axis |
| Microcontinent | Extensional faults | Shear zone |
| Oceanic crust | Anticline | Suture |
| Orogen/foldbelt | | Coastline |







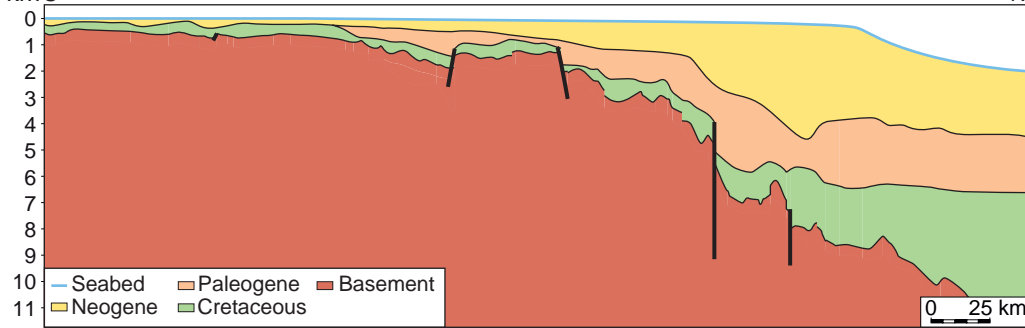
De Long Plateau

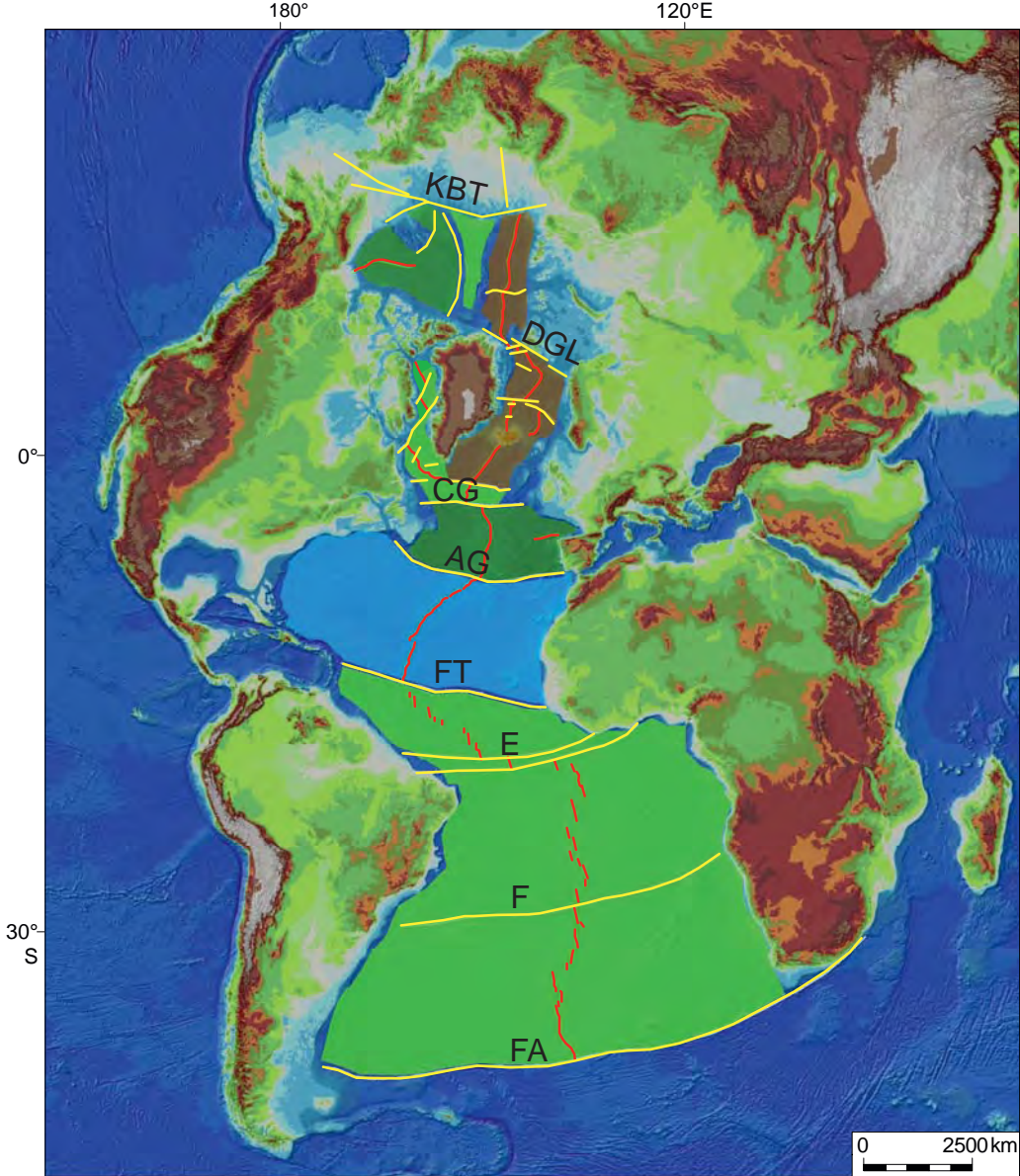
Khatanga-Bering
Transform /COB

Makarov-
Podvodnikov
Basin

km S

N





- Cenozoic
- Late Cretaceous
- Early Cretaceous
- Jurassic

- Fracture zone
- Spreading axis

0 Ma



- | | |
|---------------------------|------------------------|
| Subduction zone | Spreading axis: |
| Inactive | Active |
| Fracture/shear zone | Incipient |
| Inactive | Inactive |
| Subduction direction | Relative opening |
| COB | Oceanic crust |
| South Annui Suture | Microcontinent |
| Magmatism mainly basaltic | Orogens - active |
| Shear motion | Orogens - inactive |

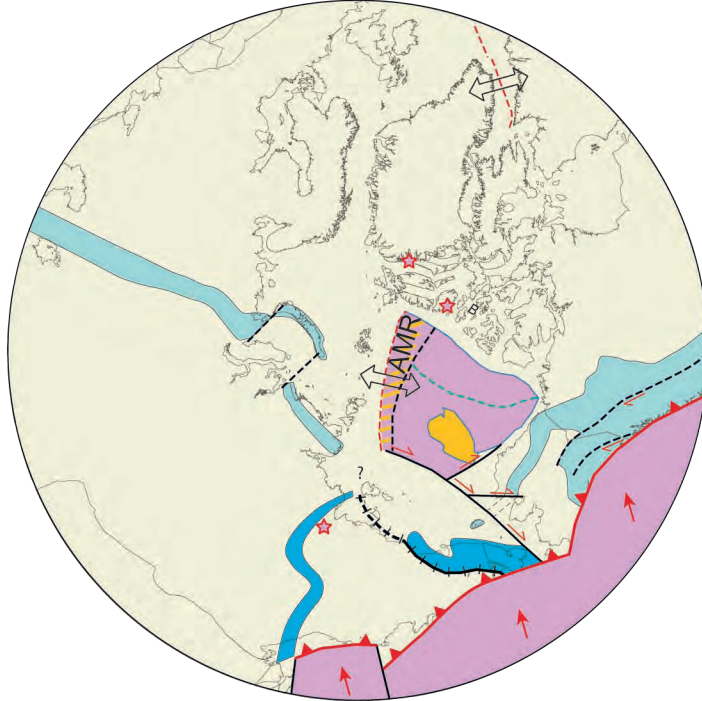
125 Ma



100 Ma



80 Ma



60 Ma



33 Ma

